



# Response of the magnetosphere–ionosphere system to sudden changes in solar wind dynamic pressure

## Global magnetohydrodynamic modeling studies of geomagnetic sudden commencements

Shigeru Fujita<sup>1,2</sup> 

Received: 26 June 2018 / Accepted: 29 April 2019 / Published online: 20 May 2019  
© Division of Plasma Physics, Association of Asia Pacific Physical Societies 2019

### Abstract

The geomagnetic sudden commencement (SC) is a plasma and magnetic field disturbance in the magnetosphere–ionosphere region, which appears as a response of this system to a sudden change in the solar wind dynamic pressures associated with shock and tangential discontinuity of solar wind. As this mechanism seems to be simple, the SC has been widely investigated based on observations in the region from the surface of the Earth to the magnetosphere. A schematic model of the SC was presented by Araki (Solar wind sources of magnetospheric ultra-low-frequency waves. American Geophysical Union, Washington, DC, pp 183–200, 1994), who compiled many observational results and theories related to this phenomenon. Recent advances in supercomputing allow us to present new numerical results including three-dimensional global current systems of the SC which cannot be obtained only by direct observations and theoretical analysis. The simulation study not only confirms the results of a previous model on the initial response of the magnetosphere–ionosphere system to solar wind changes (the preliminary impulse) but also presents new findings on dynamical processes in the magnetosphere–ionosphere system in the period following the initial response (the main impulse). Furthermore, the simulation study reveals the SC sequence in the context of break and recovery of the steady magnetosphere–ionosphere convection system. The transient flow vortex in the flank magnetosphere in the main impulse phase plays an essential role in recovering the convection system. This report describes the SC process from the viewpoint of the state transition of the magnetosphere–ionosphere compound system Tanaka (Space Sci Rev 133:1, <https://doi.org/10.1007/s11214-007-9168-4>, 2007).

---

This research was supported by JSPS KAKENHI Grant Numbers JP17K05671 and JP15H05815.

Extended author information available on the last page of the article

**Keywords** Geomagnetic sudden commencement · State transition · Magnetosphere ionosphere compound system · Global MHD simulation

## 1 Introduction

The solar wind is a plasma flow blowing outward against the solar gravitational force. With respect to the Earth, the incident solar wind flow is super-magnetosonic (Parker 1958). On the other hand, the Earth has the magnetosphere which is influenced by its magnetic field. Since the solar wind plasmas cannot penetrate into the domain of the Earth's magnetic field, a boundary called the magnetopause is formed between the solar wind and the magnetosphere (e.g., Hughes 1995). The balance between the solar wind dynamic pressure and the magnetic pressure of the magnetosphere determines the location of the magnetopause (e.g., Nishida 1978). A sudden change in the solar wind dynamic pressure causes a rapid shift of the magnetopause. Plasma and magnetic field disturbances invoked by this change propagate through the magnetosphere–ionosphere region. Magnetic storms sometimes occur as a consequence of the disturbance. The disturbance followed by the magnetic storm and that without it are referred to as the Storm Sudden Commencement (SSC) and the Sudden Impulse (SI), respectively. However, there is no fundamental difference between the SSC and the SI in terms of the initial disturbances. Therefore, the disturbances are more generally called the Sudden Commencement abbreviated by SC (Joselyn and Tsurutani 1990).

The SC studies in the twentieth century, that is, the studies before the global magnetohydrodynamic (MHD) simulations of the magnetosphere–ionosphere system (we will refer to this simulation as the global MHD simulation from this point onwards) became available, mainly described new findings by ground-based and satellite-based observations, and explained the mechanisms of observational facts based on theory and conceptualized qualitative models on global plasma behavior in the magnetosphere. In summary, the studies at that time were limited to attempting to elucidate the cause-and-effect relations of observed phenomena. The achievements of twentieth-century SC studies are summarized by Araki (1994) which will be explained in Sect. 2. In the twenty-first century, it is possible to utilize global MHD simulations that accurately solve the MHD equations in magnetosphere–ionosphere systems. Thus, this simulation study may facilitate a deeper understanding of the observational facts of the SC in quantitative manners.

We noticed that based on the MHD simulation, the SC could be understood as the transition between two steady states of the magnetosphere–ionosphere systems corresponding to two constant solar wind conditions before and after the sudden change of the dynamic pressure. The steady magnetosphere–ionosphere coupling convection is established under the constant solar wind condition. Therefore, the rest of this section explains the process of convection based on Tanaka (2007), before we outline the achievements of the most recent SC studies in the next sections.

First, we explain the concept of convection as used in the twentieth century. It is known that the ground magnetic variations in the polar region, on average, can be described as a clockwise ionospheric convection cell in the afternoon sector and

an anti-clockwise ionospheric convection cell in the morning sector (Nagata and Kokubun 1962). This fact implies that there is an anti-sunward plasma flow in the polar cap region and a sunward flow in the lower latitude regions. This ionospheric flow pattern corresponds to negative/positive electric potential in the afternoon/morning sector in the northern hemisphere. Since the ionospheric electric field is connected to the magnetospheric electric field through the perfectly conducting magnetic field lines, the integrated large-scale convection called the magnetosphere–ionosphere coupling convection is established. Thus, the magnetic and particle flux along with the magnetic field lines in the magnetosphere are transported from the dayside to the nightside in the noon-midnight meridian and returns to the dayside again in the lower latitude region. To explain this convection, Dungey (1961) proposed a conceptual model called the Dungey cycle based on magnetic reconnection between the interplanetary magnetic field (IMF) and the magnetospheric magnetic field. According to this model, when the IMF is southward, for example, the magnetospheric closed magnetic field lines which are merged with the IMF by reconnection in the daytime magnetopause is open, and the merged field lines are transported toward the magnetospheric tail. In the tail, reconnection occurs again to form closed magnetic field lines. The closed field lines are transported towards the dayside magnetosphere. Finally, the magnetosphere convection cycle is completed. When the IMF is northward with a non-zero east–west component, the ionospheric convection pattern is deformed from the two-cell convection pattern for the southward IMF condition; it exhibits a large round-shape cell in the polar cap region where the magnetic field is open, and a crescent-shaped cell in the lower latitude side of the round cell (Friis-Christensen et al. 1985). Even in the case of the northward IMF, the magnetosphere–ionospheric convection is defined as fundamentally similar to that of the conceptual diagram presented by Dungey (1961) and Maezawa (1976).

The new understanding of convection based on the global MHD simulations (the convection model used in the twenty-first century) was introduced relatively recently (Tanaka 2007). There must be a current system connecting the magnetosphere and the ionosphere because the magnetosphere–ionosphere coupling convection requires an ionospheric electric field. This current system is the Region 1 field-aligned current (FAC) system (upward in the afternoon side, downward in the morning) (Iijima and Potemra 1976). One of the significant advantages of the global MHD simulation is that it facilitates accurate 3D imaging of electric current lines. Thus, we obtain the 3D pattern of the Region 1 FAC system from the simulation. A dynamo sustaining the Region 1 FAC system is required because the ionosphere is dissipative. The simulation also reveals that the dynamo appears in the cusp–mantle region. In addition, the most essential finding based on the simulation is that the dynamo ( $\mathbf{E}_\perp \cdot \mathbf{J}_\perp < 0$  where  $\mathbf{E}_\perp$  and  $\mathbf{J}_\perp$  are the electric field vector perpendicular to the magnetic field and the perpendicular electric current vector, respectively) is driven by energy conversion from the thermal energy ( $\mathbf{v}_\perp \cdot \nabla P < 0$ , where  $\mathbf{v}_\perp$  and  $P$  are the convection flow vector and the thermal pressure, respectively) (Tanaka 1995). From the conceptual model by Dungey (1961), the convection has been regarded to be driven directly by the magnetic tension force caused by reconnection in the dayside magnetopause (e.g., Baumjohann and Treumann 1997). On the other hand, the simulation also reveals that the magnetic tension force does not directly drive the

magnetosphere–ionosphere coupling convection, as recently reported (Tanaka et al. 2016). Thus, there is still inconsistency regarding the convection generation mechanism between the conceptual model and the MHD simulation. This issue will be studied in a future investigation.

Finally, deep insight into the simulation results leads to the concept of the magnetosphere–ionosphere compound system, which cannot be easily obtained from only observations (Tanaka 2003). In the compound system, all elementary processes including the driving of the FAC dynamo, the formation of plasma regimes (e.g., high-pressure plasmas in the cusp), the magnetospheric current (the Region 1 FAC system), the ionospheric current, the ionospheric potential, and the plasma convection, must satisfy the global consistency. That is to say, the dynamo drives the Region 1 current; the Region 1 current induces the ionospheric electric field, which must be consistent with the magnetospheric convection by the line-tying effect; the high-pressure plasmas in the cusp region are associated with the magnetospheric convection; the dynamo is driven in the cusp–mantle region where  $\mathbf{v}_\perp \cdot \nabla p < 0$ . Note that the solar wind condition is constant. (The solid Earth under the ionosphere with the neutral atmosphere in between does not have a direct influence on the physical process of the magnetosphere–ionosphere compound system. This is because the FAC that induces the ionospheric electric field does not penetrate into the neutral atmosphere. Indeed, the ratio of the electric field of the reflected Alfvén wave to that of the incident Alfvén wave is independent on the Earth's properties because it is  $(\Sigma_A - \Sigma_p)/(\Sigma_A + \Sigma_p)$  when the spatial scale of the convection ( $\sim 10^4$  km) is much larger than the height of the ionosphere ( $\sim 10^2$  km) where  $\Sigma_A$  and  $\Sigma_p$  are the Alfvén conductance ( $= \mu_0 V_A$  where  $\mu_0$  and  $V_A$  are vacuum magnetic permeability and the Alfvén speed) and the Pedersen conductance, respectively, after Nishida 1978.) In other words, the convection system cannot be understood in terms of the unilateral cause-and-result relations of elementary processes. The compound system can be regarded as the state of the magnetosphere–ionosphere system corresponding to the specific condition of the solar wind.

It is noted that the compound system described above exhibits a unique state of the steady magnetosphere–ionosphere system. The sudden change in the solar wind dynamic pressure will temporally break the global consistency of the compound system as noted before. Therefore, a new study is needed to understand the SC as the global magnetosphere–ionosphere process in which the broken consistency recovers after the solar wind change. We will investigate which parts of SC disturbances correspond to the break and recovery of global consistency. This paper describes both the simulation works that confirm previous theoretical predictions in a quantitative manner, as well as the new concept of the SC based on the compound system.

The rest of this paper is structured as follows. Section 2 summarizes the observational facts on the SC that were primarily reported after Araki (1994). The SC current system in the magnetosphere based on observations will be presented in this section. The section also describes the debate on the global transmission of the SC signal in detail. Section 3 examines the simulation results based on global MHD simulations. In addition, this section includes simulation works on the MHD waves associated with the SC. Section 4 describes several recent topics, mainly on the simulation studies of the SC. Section 5 summarizes the main conclusions.

## 2 The SC model compiled from the observations

When we investigate global phenomena such as the SC in the magnetosphere–ionosphere compound system, it is essential to elucidate the electric current system in the magnetosphere–ionosphere region. Therefore, this section mainly summarizes the observational facts related to the theories on the current system of the SC before the global simulation was widely available. In addition, it is characteristic that the SC signals seem to appear on the ground almost simultaneously from the polar region to the magnetic equator. The first part of this section describes the observational facts used for identification of the ionospheric FAC associated with the SC. Next, we describe the global transmission of the SC signal. The last section provides an explanation of the theory and the model of the SC current system compiled from the observational facts before the global simulation became available.

### 2.1 The observational facts relating to the SC current system

The SC usually exhibits a sudden increase in the northward component of the ground magnetic field with a time scale of several minutes at the mid- and low latitude (Araki 1994). The ground magnetic variations associated with the SC show different features according to latitude. The global features of the ground magnetic field variations of the positive SC (the SC triggered by a sudden increase in the solar wind dynamic pressure) are summarized by Araki (1994) as shown in Fig. 1.

The dawn-to-dusk (eastward) Chapman–Ferraro current flowing in the magnetopause suddenly increases at the SC because it balances with the sudden increase in the solar wind dynamic pressure. As a result, the northward component of the ground magnetic field increases as shown in panels (c) and (d) of Fig. 1. This magnetic variation is termed the DL (= Disturbance of Low latitude) component because this variation is significant at low latitudes. On the other hand, the ground magnetic signatures associated with the SC at higher latitudes of approximately  $60^{\circ}$ – $70^{\circ}$  (the auroral latitudes) exhibits bipolar variations as shown in panels (a) and (b) of Fig. 1. The first magnetic field change is called the preliminary impulse (PI), and the subsequent reverse change is called the main impulse (MI). This bipolar magnetic field variation is termed DP (= Disturbance of Polar latitudes) because a magnetic field variation in the polar region mainly consists of this variation. The SC magnetic field variation observed at an arbitrary latitude on the ground is a mixture of DP and DL. The contribution of DP/DL becomes larger in the higher/lower latitudes. However, the DP also appears clearly again in the dayside magnetic equator as shown in Fig. 1.

The bipolar geomagnetic variations of DP indicate that the ionospheric twin vortex of plasma flows both in the morning side and in the afternoon side. This vortex system moves from dayside to the nightside in the auroral latitude. It is associated with the preceding upward/downward FAC and the flowing downward/upward one in the afternoon/morning side (Araki 1994). It has been noted that this twin vortex which travels nightward is similar to the traveling convection vortices (TCV) (Glassmeier et al. 1989). However, the SC is a global phenomenon associated with

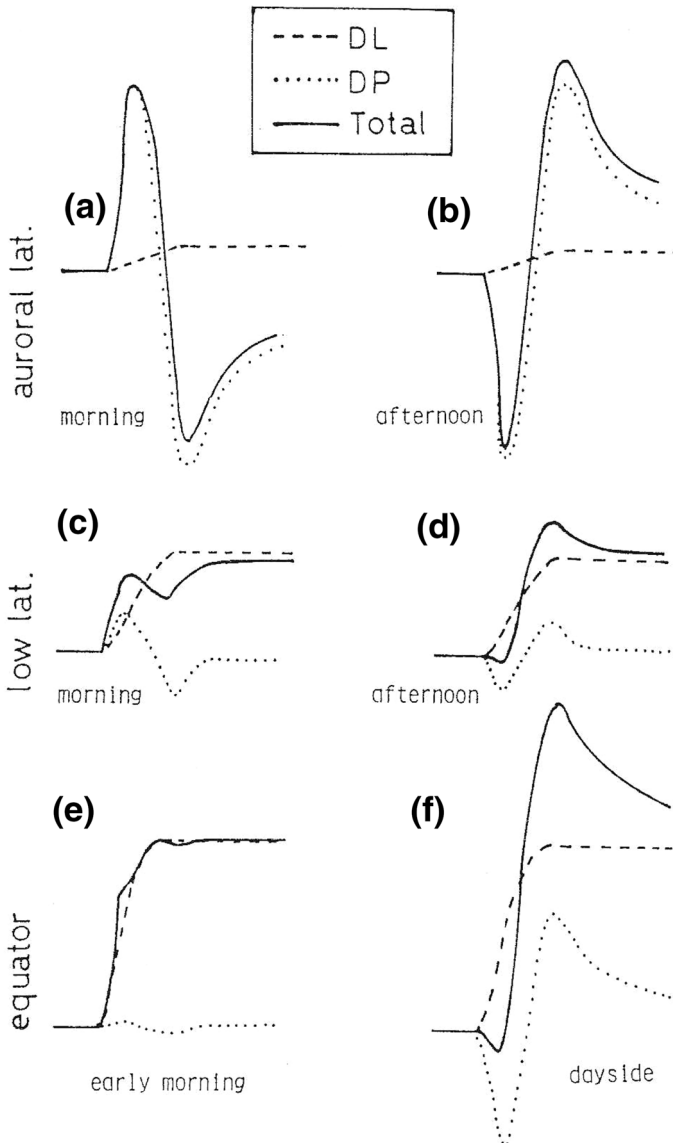


**Fig. 1** Typical variations of the north-south ground magnetic component (H-component) associated with the SC **a, b** at the auroral latitudes ( $60^{\circ}$ – $70^{\circ}$ ), **c, d** at the lower latitudes ( $20^{\circ}$ – $50^{\circ}$ ), **e, f** at the geomagnetic equator ( $< 1^{\circ}$ ). Thick, broken, and dotted curves in each panel represent the total, DL, and DP component of the SC ground magnetic variations. After Araki (1994)

the DP variation in the polar region and the DL variation in the mid- and low-latitude regions. On the other hand, the TCV is regarded to be localized in the polar region (Kivelson and Southwood 1991; Kataoka et al. 2004). We should discriminate between the SC and the TCV.

## 2.2 Global transmission of the SC signal

In the dayside magnetic equator, the DP component becomes dominant as shown in the panel (f) of Fig. 1. Araki (1994) also noted an almost simultaneous onset of the DP variations in the polar region and at the magnetic equator. The simultaneous onset is explained as follows. The height-integrated ionospheric conductivity tensor ( $\Sigma$ ) is expressed as

$$\Sigma = \begin{pmatrix} \Sigma_{xx} & \Sigma_{xy} \\ \Sigma_{yx} & \Sigma_{yy} \end{pmatrix}, \quad (1)$$

where  $x$  and  $y$  mean the northward, and eastward, respectively. At the magnetic equator, enhanced  $\Sigma_{yy}$  induces enhanced east–west current from the east–west electric field (the Cowling effect) (Fejer 1964). Thus, an even weaker electric field in the ionosphere can induce significant magnetic variation at the equator compared with the negligibly small variation in the mid-latitude region. Consequently, the simultaneous onset of the DP at a higher latitude and at the magnetic equator suggests instantaneous global transmission of the electric field induced by the high-latitude FAC which drives the DP magnetic variations at the auroral latitudes. It has been noted that the horizontal propagation of the fast magnetosonic wave within the ionosphere does not explain the simultaneous occurrence because the fast wave suffers severe attenuation in horizontal propagation (Kikuchi and Araki 1979a). Kikuchi and Araki (1979a) also mentioned that the ionospheric F-layer waveguide for the fast magnetosonic wave cannot transport signals with frequencies lower than the cutoff frequency ( $\sim 1$  Hz). The Earth–ionosphere waveguide transmission of the  $TM_0$  electromagnetic signal shown in Fig. 2 is the unique physical mechanism of the global transmission of the electric field applied to high latitudes (Kikuchi et al. 1978; Kikuchi and Araki 1979b). (The  $TM_0$  mode is the lowest order waveguide mode of the electromagnetic wave polarized in the east–west direction as shown in  $\mathbf{B}$  in Fig. 2). Therefore, the global ground magnetic variations of the SC are driven by both the global ionospheric electric field caused by the magnetospheric FACs flowing into/out of the polar region (DP) and the enhanced Chapman–Ferraro current (DL). Tsunomura and Araki (1984) calculated the global distribution of the ionospheric electric field induced by a pair of FACs during the morning and afternoon in the high-latitude ionosphere using the realistic ionospheric conductivity model. (Tsunomura (1999) presented results for the enhanced ground magnetic variation at the geomagnetic equatorial region due to the Cowling effect, based on numerical code which was improved to address the ionospheric conductivity structure in the magnetospheric equator carefully.) These modeling studies were able to well reproduce global magnetic variations. Therefore, Araki (1994) concluded that the SC signatures in the polar region and in the equatorial region are caused by the ionospheric electric field induced by the upward and downward pair of the FACs at higher latitudes. Recently, Kikuchi et al. (2016) reinforced this model by elucidating that the global electric field associated with the SC is the potential field produced by the FAC injected into the polar region.

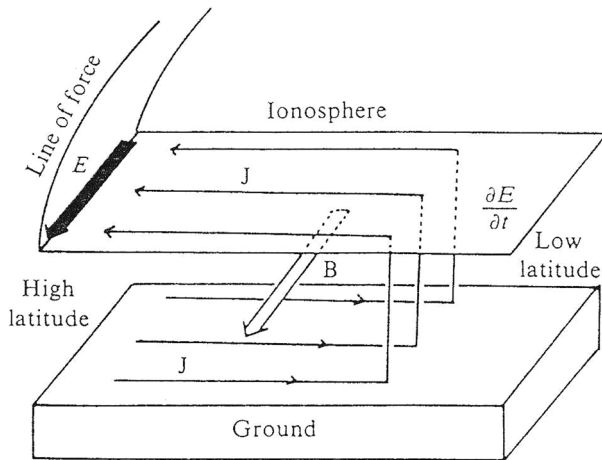


**Fig. 2** Horizontal transmission of the polar ionospheric signal injected from the magnetosphere to the lower latitudes. The polar ionospheric signal is denoted as  $E$  (the east–west electric field). The time-dependent  $E$  induces the 3D current system ( $J$ ) in the ionosphere–atmosphere–ground region. The vertical displacement current in the atmosphere ( $\propto \partial E/\partial t$ ) propagates to the lower latitudes at the speed of light. This current system generated the east–west magnetic field ( $B$ ). This is the electromagnetic structure of the  $TM_0$  mode in the ionosphere–atmosphere–ground waveguide. After Kikuchi et al. (1978)

An argument has been presented with regard to the transmission of the PI signal from the polar region to the lower latitude region. Yumoto et al. (1997) reported on the non-zero arrival time difference of the peak of the PI signal from the higher latitude station to the lower latitude one using ground magnetic data with higher time resolution. Later, Chi et al. (2001) presented that the peak of the ground magnetic variation in the PI phase arrives first at the plasmapause latitudes by investigating the latitudinal change of the arrival time. They explained this observational fact by the theory presented by Tamao (1964a) in which the MHD wave generated in the magnetopause propagates in the magnetosphere directly to the ionosphere (the MHD wave propagation theory in the PI phase will be explained in Sect. ). Since the wave speed (the Alfvén speed) is increased in the plasmapause region, the wave passing the plasmapause arrives the ionosphere first. Thus, they called this propagation time the Tamao travel time. Later, Chi and Russell (2005) advocated “the magnetoseismology” because the plasma density distribution in the magnetosphere may be estimated using the Tamao travel times obtained at globally distributed ground stations, similar to the field of seismology. Here, we note that the simultaneous onset of the SC (Araki 1977) was investigated based on the onset time of the ground magnetic variation, whereas, the arrival time difference (Yumoto et al. 1997; Chi et al. 2001) was detected from the peak time of the PI signal. Therefore, both models discuss transmission/propagation of the SC signals based on the different phase of the SC ground magnetic variation. Thus, the Earth–ionosphere waveguide model and the MHD wave propagation model may not be exclusive. The appearance of the enhanced PI magnetic signal at the magnetic equator and the near-simultaneous onset of the PI from the polar region to the magnetic equator strongly



suggest horizontal transmission of the polar electric field in the Earth–ionosphere waveguide. Therefore, it is reasonable to conclude that the waveguide propagation model (Kikuchi et al. 1978; Kikuchi and Araki 1979b) induces the global electric field at the SC and the corresponding ground magnetic field variations. The fact that the observed global distribution of the ionospheric electric field is consistent with the electric field produced by the FAC in the polar region (Kikuchi et al. 2016) also support this model. On the other hand, the arrival time gap as determined from the maximum amplitude of the PI signal at the plasmopause latitudes suggests direct propagation of the MHD waves from the magnetopause to the ground (Chi et al. 2001, 2002). It would be better to suggest that the ground signals that seem to propagate from the magnetosphere (Chi et al. 2001) are superimposed on the SC field produced by the Earth–ionosphere waveguide process. Last, we note that Yumoto et al. (1997) theoretically calculated the intensity of the electric field vertical to the ground associated with the  $TM_0$  mode in the atmosphere using the realistic atmospheric electric conductivity. As a result, the electric field was estimated to be very large ( $10^2$  V/m for the SC with  $\sim 1$  nT). However, they did not find an enhanced vertical atmospheric electric field. This problem may be a future issue of the Earth–ionosphere waveguide model.

### 2.3 The theory and the model of the SC current system

Let us summarize the previous theoretical research on the DP of the SC. The disturbance associated with the PI is considered to be an MHD wave caused by the sudden change in the solar wind dynamic pressure compressing the entire magnetosphere. Tamao (1964a, b) and Nishida (1964) first theoretically considered the propagation of the MHD wave driven by the sudden change in the solar wind dynamic pressure. Because the theory presented by Nishida (1964) is essentially the same as Tamao (1964a, b), the results by Tamao (1964a, b) are summarized here.

Tamao (1964a, b) considered the cold MHD wave theory in uniform plasmas. Based on theoretical analysis, Tamao (1964a) elucidated that localized compression of the magnetopause triggers the isotropic mode MHD wave (the compressional wave/the fast magnetosonic wave) propagating isotropically. This isotropic mode couples with the transverse mode MHD wave with FAC (the Alfvén wave) when the isotropic mode propagates across magnetic field lines. Subsequently, Tamao (1964b) presented the model that the isotropic mode generated by localized compression of the magnetopause induces the localized mode that propagates to the ionosphere as the FAC. (This theory suggests that the MHD wave converted from the isotropic mode to the localized mode on the field line in the plasmopause region tends to arrive at the ionosphere first because the Alfvén speed is increased in this region. Chi et al. (2001) employed this theory to explain the observed arrival time difference of the PI signal.) Let us consider the amplitude of the wave generated by the sudden compression of the magnetopause. Since Tamao (1964a) assumed a uniform magnetosphere, the isotropic mode from a point source has a geometrical attenuation of  $1/r$ , where  $r$  is the distance from the wave generation center. In this case, the localized mode converted from the isotropic mode on the field line inside

the magnetosphere has reduced intensity because of geometrical attenuation of the isotropic mode from the source on the magnetopause to the field line in the magnetosphere. Therefore, the FAC intensity in the ionosphere gradually decreases as it moves away from the magnetopause to the lower latitudes. These theories lead to the conclusion that the FAC in the ionosphere will have a maximum intensity at the magnetopause latitude. However, observations show that the FAC of the PI appears at latitudes well inside of the magnetopause (the auroral latitudes) (Araki 1994). Finally, Tamao (1965) showed that the isotropic mode wave propagating in a spatially non-uniform field transforms into the transverse mode wave. In this theory, the isotropic mode wave generated by the magnetopause compression effectively converts to the transverse mode wave in the region where the background plasma and/or the magnetic field intensity are strongly non-uniform. Then the FAC is enhanced at that latitude. The plasmopause is a candidate for a location with enhanced non-uniformity. Then the PI signal appears at lower latitudes than that of the magnetopause.

Following the aforementioned theoretical investigations, Araki (1994) presented a schematic picture of the three-dimensional PI current system of the magnetosphere–ionosphere region (Fig. 3a). When the solar wind dynamic pressure suddenly increases, the magnetopause is pushed inward. In reaction to the increasing pressure in the magnetopause, the Lorentz force ( $\mathbf{J}_M \times \mathbf{B}$ ) increases, i.e., the magnetospheric magnetic field increases ( $\mathbf{b} \rightarrow \mathbf{B}$ ). This magnetic field variation propagates in the magnetosphere as an MHD wave. The polarization current  $\mathbf{J}_p$  flows perpendicularly

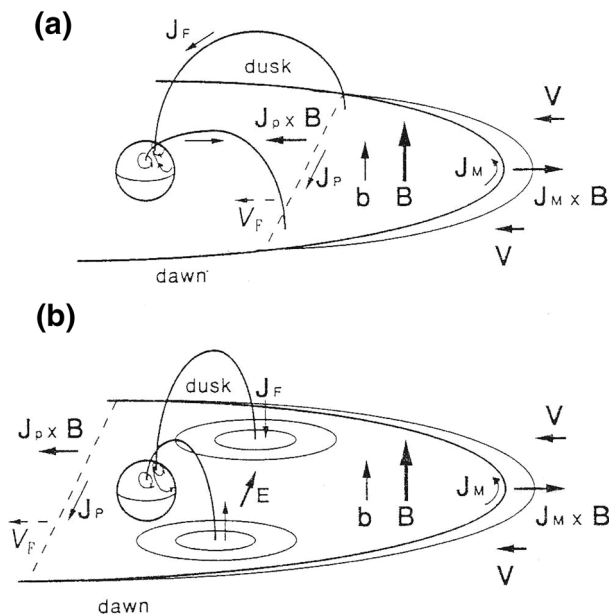


**Fig. 3** **a** Magnetospheric current system in the PI phase and **b** the MI phase. The enhanced solar wind dynamic pressure is balanced by the intensified Lorentz force ( $\mathbf{J}_M \times \mathbf{B}$ ), where  $\mathbf{J}_M$  is the magnetopause current (the Chapman–Ferraro current). The magnetic field intensity in the dayside magnetosphere also increases ( $\mathbf{b} \rightarrow \mathbf{B}$ ) at the SC. See the text for detail. FACs generated in the magnetosphere induce the ionospheric potential in both phases. After Araki (1994)

to the magnetic field line on the wavefront. A component of  $\mathbf{J}_p$  is converted into the FAC in the magnetosphere, with currents moving upward in the morning and downward in the afternoon. In this PI model, the moving velocity of the FAC position in the ionosphere is determined by the magnetosonic velocity in the magnetosphere.

Next, the current system of the MI proposed by Araki (1994) is shown in Fig. 3b. Araki (1994) considered that the MI signal is produced in the magnetospheric state after the magnetosonic wavefront was dissipated. Thus, the steady magnetospheric convection with the upward/downward FACs in the afternoon/morning sectors is as shown in the figure. These FACs belong to the Region 1 FAC system (Iijima and Potemra 1976). The PI current system model is constructed after the process based on the theory of Tamao (1964b). However, the MI current system model is phenomenological. Moreover, the ground magnetic field variations in the MI phase do not exhibit a stationary behavior as shown in Fig. 1. Araki (1994) did not, however, clearly explain the source of the MI current system. Therefore, the physical processes in the MI phase were not completely elucidated by Araki (1977). The current system of PI and that of MI shown in Fig. 3 are models of SC constructed on the basis of observation data before the global MHD simulation was utilized.

### 3 Modeling studies of the SC

Since the 1990s, global MHD simulations have been used to reproduce plasma disturbances and magnetic field variations of the entire magnetosphere–ionosphere region driven by solar wind changes. The global MHD simulation not only facilitates a deeper understanding of the causality issues of observational phenomena of the SC in a quantitative manner but also stimulates the consideration of the fundamental physical processes responsible for the observational facts. This section provides a summary of the new findings afforded by global MHD simulations in SC studies. In the last part of this section, we will summarize the MHD wave simulation studies because it covers areas of SC research which cannot be precisely treated using the global MHD simulation.

#### 3.1 The SC study based on the global MHD simulation

The early simulation studies concentrated on the reproduction of observed phenomena instead of attempting to establish deep insight into the physical processes of the SC. The first simulation work on the SC was performed by Slinker et al. (1999) who presented the magnetospheric and ionospheric plasma disturbances in the event of a sudden increase of the solar wind density using the global MHD simulation code developed by Fedder and Lyon (1987). They employed the tangential discontinuity (TD) in the typical solar wind with the northward IMF ( $B_y = B_z = 3.53$  nT,  $v_x = -400$  km/s) and a sudden increase in the plasma density (5/cc→20/cc). It should be noted that the ionosphere has only a uniform Pedersen conductivity. As such, they did not discuss the ground magnetic variations. Their simulation reproduced the temporal changes of the convection flow patterns in the magnetospheric

equatorial plane and those in the ionosphere, as well as the changes of the ionospheric electric potential. These reproductions are very similar to those observed at the SC event. However, they insisted that the flow vortex they reproduced is categorized as a traveling convection vortex (TCV) (Glassmeier et al. 1989). This conclusion is not valid because the TD and the fast shock (FS) in the solar wind generate the global disturbances from the polar region to the equatorial region, which is not consistent with the definition of TCV (Kivelson and Southwood 1991; Kataoka et al. 2004). Also, Fujita et al. (2003a) insisted that the ionospheric disturbances simulated by Slinker et al. (1999) should be categorized with the disturbances associated with the SC. Subsequently, Keller et al. (2002) investigated the magnetospheric response to the gradual increase in the solar wind density from 2.5/cc to 10/cc using the MHD simulation code developed by Gombosi et al. (1994). The solar wind speed was 340 km/s, and the IMF was due north ( $B_z = 1$  nT). Keller et al. (2002) first showed the movement of the FAC distributions from the dayside to the nightside in the ionosphere and the corresponding potential distributions. (The FAC pattern is anti-symmetric with respect to the noon-midnight meridian because the IMF is due north.) The distribution of the potential is similar to the observed distribution by Moretto et al. (2000). However, their results are not completely correct because the ionosphere only has a Pedersen conductivity.

The magnetosphere and the ionosphere couple to each other in the magnetosphere–ionosphere compound system. Therefore, not only the magnetosphere, but also the ionosphere has to be treated correctly. The first SC study based on the more realistic magnetosphere–ionosphere system was performed by Fujita et al. (2003a, b). The ionosphere has both the Pedersen and Hall conductivities after Tanaka (1999). These two publications also investigated physical processes in the magnetosphere–ionosphere region caused by the TD associated with the sudden increases in the solar wind density (10/cc→25/cc). They employed the typical northward IMF condition ( $B_y = -2.5$  nT,  $B_z = 4.3$  nT,  $v_x = -350$  km/s) in the simulation. This code was developed by Tanaka (1994). Because the global MHD simulation sets the lower boundary of the magnetosphere at the altitude of 3Re due to numerical difficulties, the treatment of the ionosphere in the simulation is usually restricted to the region with latitudes higher than about 55°. Therefore, only the DP is discussed by Fujita et al. (2003a, b).

Let us introduce a validation of the simulation result. The ionospheric process reflects all magnetospheric processes in the magnetosphere–ionosphere compound system. Therefore, it is essential to examine how the ground magnetic variations are similar to the observed ones. The magnetic variations observed in the high latitudes exhibit two phases: the PI phase and the MI phase as noted in Sect. 2. The global MHD simulation indeed reproduces sufficiently the high-latitude magnetic variations associated with the SC as shown in Fig. 4, which are very similar to the observed DP variations shown in Fig. 1. In addition, the observed H-component variation in Alaska in the evening time shown in Fig. 5 is quite similar to the calculated H-component variation in Fig. 4. As for the D component, the waveforms of the observed and calculated variations are rather different, but both show positive and negative bipolar variations in the latitudes between 70° and 80°. Since the simulation treats an idealized solar wind condition with constant IMF and constant solar wind

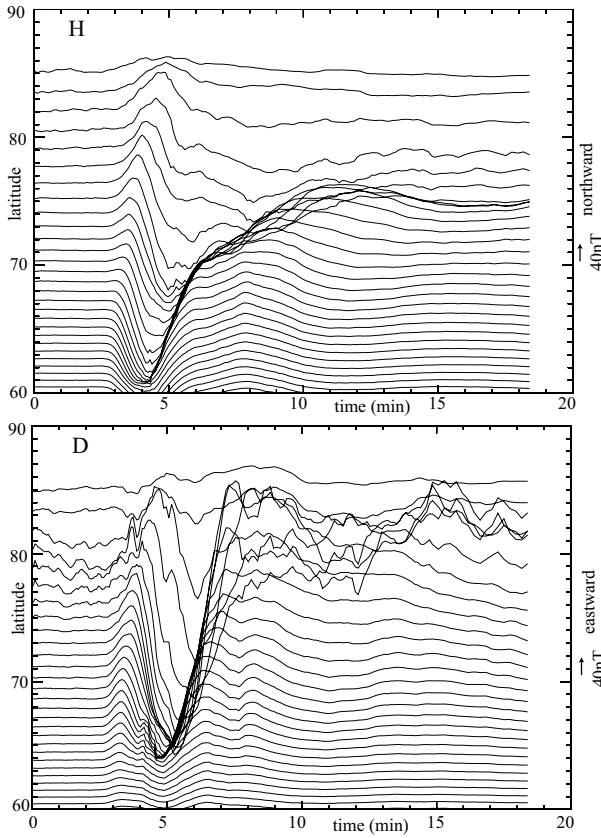
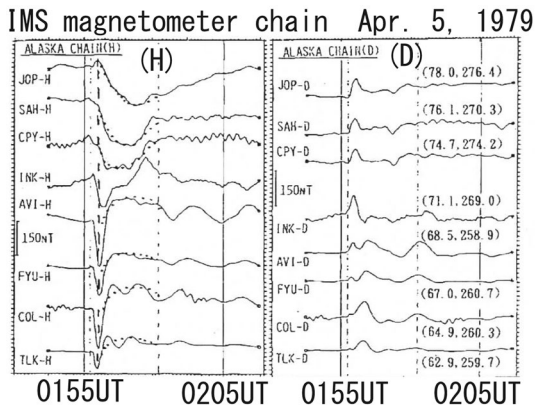


**Fig. 4** Latitudinal distribution of temporal changes in ground magnetic variations in the northern polar region at 15 hMLT driven by the sudden increase in the solar wind dynamic pressure obtained by the global MHD simulation. The distances between the neighboring ticks along the vertical axis denote 40 nT. After Fujita et al. (2003a)

**Fig. 5** Latitudinal distribution of temporal changes in ground magnetic variations observed on Apr. 5, 1979, in the IMS Alaska chain. This chain is located in the evening sector. After Araki (1994)



speed and a sudden increase in the density, the simulation results do not correspond completely to the observed one. It should be noted that time in the simulation results is counted from the time when the density pulse in the solar wind starts at  $x=18R_e$  upstream of the bow shock. Thus, this result guarantees that the global MHD simulation by Fujita et al. (2003a, b) is capable of manifesting the mechanisms that drive the current systems connecting the magnetosphere and the ionosphere.

It is noted that Slinker et al. (1999), Keller et al. (2002), and Fujita et al. (2003a, b) use different kinds of simulation codes. However, the ionospheric electric field patterns shown in these papers are in common with the result of Fujita et al. (2003a, b). Therefore, this fact supports that the calculation results by these papers are regarded to be reliable. The grid sizes used by Keller et al. (2002) and by Fujita et al. (2003a, b) are about  $0.25R_e$ . The subsequent global MHD simulation research uses the grid sizes equal to or less than this. Thus, the simulation works dealt with in this paper use sufficient fine meshes. It is noted that all global MHD simulations treated in this paper do not have the plasmasphere and the lower boundary of the magnetosphere is at  $2\text{--}3R_e$ . Thus, the global MHD simulation is not capable of reproducing near-Earth plasma behaviors. The electric current in the lower boundary of the magnetosphere flows into the ionosphere along the magnetic field line, and the ionospheric electric field induced by this field-aligned current is mapped into the electric field in the lower boundary of the magnetosphere. Except for some simulation studies (Slinker et al. 1999; Keller et al. 2002; Kim et al. 2009), the ionospheric Pedersen and Hall conductivities are determined from the solar radiation, precipitation of electrons (the upward FAC), and pressure/temperature at the lower boundary of the magnetosphere.

Since the SC has the two phases of PI and MI, it is reasonable to discuss the physical processes of the SC in two separate components. Following the earlier three papers, there have been many publications on the SC based on global MHD simulations. Here, we summarize the results of these simulation studies with respect to the physical processes of the PI phase and the MI phase in Sects. 3.1.1 and 3.1.2, respectively. In particular, we discuss the SC from the viewpoint of the state transition of the magnetosphere–ionosphere compound system. Other topics will be described in Sect. 4.

### 3.1.1 The PI phase

Fujita et al. (2003a) confirmed that the magnetospheric disturbances in the PI phase are associated with the MHD waves based on simulation analysis. This suggests that the magnetosphere responds temporally to the sudden change of the solar wind dynamic pressure in the PI phase. Therefore, we do not need to consider the magnetosphere–ionosphere compound system for the study of the PI process. The numerical studies of the PI process are mainly conducted to confirm the previously proposed concepts (Araki 1994).

The current system of the PI phase in the ionosphere obtained by the simulation is presented by Fujita et al. (2003a). This paper shows the ionospheric FAC distribution and the electric potential distribution in the polar region with latitudes higher than  $60^\circ$  in the northern hemisphere. Figure 6 shows the ionospheric FAC

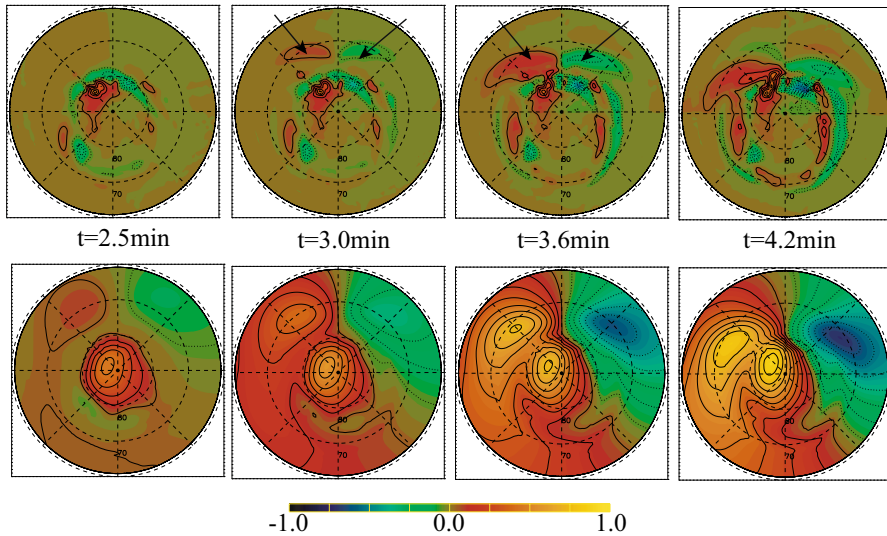


**Fig. 6** (Top row) Time changes of the ionospheric FAC distribution and (bottom row) of the electric potential for the PI phase in the northern polar region for latitudes higher than  $60^\circ$ . Positive and negative FACs denote downward and upward currents, respectively. The black arrows in the figures denote the PI current. The top of each panel corresponds to 12 hMLT. The FAC and the potential are normalized to  $5 \times 10^{-7}$  A/m<sup>2</sup> and 50 kV, respectively. This figure is a colored reproduction of Fig. 1 of Fujita et al. (2003a)

distribution and the electric potential distribution in the region with latitudes higher than  $60^\circ$ . This figure is a colored version of Fig. 1 from Fujita et al. (2003a). It shows that the downward/upward FAC appears in the afternoon/morning at the latitude of approximately  $70^\circ$  in the dayside and moves to the nightside along with the sudden increase of the solar wind dynamic pressure, as represented by the black arrows. The current induces a positive/negative electric potential in the ionosphere on the afternoon side/morning side when moving from dayside to nightside. This pattern of the ionospheric FAC and potential during the SC event are consistent with observation (e.g., Engebretson et al. 1999). The temporal changes of the FAC pattern and the electric potential shown here are consistent with the results by Keller et al. (2002). Yu and Ridley (2009) showed that the ionospheric signatures in the PI phase for the southward IMF conditions are the same as those for the northern IMF conditions.

The essential merit of the global MHD simulation is that the simulation produces the 3D grid point values in the magnetosphere–ionosphere region. Fujita et al. (2003a) (the northward IMF case) and Yu and Ridley (2009) (the southward IMF case) employed this merit to show snapshots of the magnetospheric three-dimensional current system in the PI phase. Figure 7 shows the magnetospheric PI current system at  $t = 3.0$  min when the FAC of the PI phase starts to expand toward the nightside (Fujita et al. 2003a). This figure shows that the Chapman–Ferraro current flowing along the dayside magnetopause converts to the magnetospheric current which flows along the wavefront of the fast magnetosonic wave triggered by

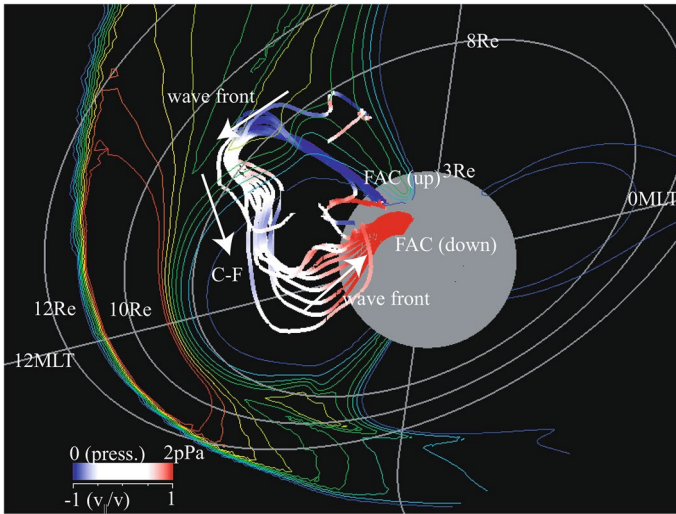


**Fig. 7** A 3D illustration of the PI current system at  $t = 3.0$  min as seen from the afternoon in the high-latitude northern hemisphere. The color contours show the pressure in the noon meridian plane. The colors of the current lines indicate  $v_{\parallel}/v$  with red, white, and blue for parallel, perpendicular, and anti-parallel to the magnetic field lines, respectively. The gray sphere represents the inner boundary of the simulation at  $r = 3R_e$ . The dawn-to-dusk magnetospheric current corresponds to the magnetopause current (the Chapman–Ferraro current). This current connects with the current to/from the inner magnetosphere in the dawn/dusk region. The currents in the dawn and dusk regions are the wavefront of the fast magnetosonic wave driven by the sudden compression of the dayside magnetosphere. This wavefront current is converted to the FAC. This figure is a reproduction of Fig. 7 of Fujita et al. (2003a)

the sudden compression of the magnetopause and converts to the downward FAC in the afternoon side. (The current flows in the opposite direction in the morning side.) This current system is in agreement with the PI current system (Fig. 3a) presented by Araki (1994). The issue is then to explain how the field-perpendicular Chapman–Ferraro current flowing in the magnetopause bends to become the FAC that connects with the ionosphere. Since the Chapman–Ferraro current does not show direct transition into the FAC in the simulation, it is necessary to investigate how the perpendicular current along the wavefront of the fast magnetosonic wave is converted into the FAC in the magnetosphere.

The simulation indicates that the PI current system shows the wave behavior because the inertial force is dominant in the dayside magnetosphere in the PI phase (Fujita et al. 2003a). Yu and Ridley (2011) also showed that the inductive  $E_y$  propagates through the magnetosphere. The presence of the inductive electric field implies that the wave plays an essential role in the PI phase. (The PI phase is referred to as the  $E_y$  phase.) Fujita et al. (2003a) explained the mechanism that produces the FAC of the PI current system by mode conversion from the fast magnetosonic wave to the Alfvén wave based on the non-uniformity of the medium (Tamao 1965). Such non-uniformity appears in the plasmopause where the Alfvén speed changes spatially. Therefore, the plasmopause is a candidate location where fast magnetosonic waves are converted to Alfvén waves with the FAC. However, because the plasmopause



usually exists at latitudes below  $60^\circ$ , this assumption does not seem to explain the simulation results. This discrepancy can be attributed to the fact that the mode conversion theory proposed by Tamao (1965) assumes cold plasma. In this case, only the spatial change of the Alfvén speed results in spatial non-uniformity. On the other hand, since plasma  $\beta$  is finite in the outer magnetosphere region in the simulation, the FAC can be generated in the boundary of different plasma  $\beta$  regimes (Tanaka 2007). In the boundary between the finite- $\beta$  plasma and the low- $\beta$  plasma (cold plasma), a magnetic shear is generated as shown in Fig. 2 of Tanaka (2007). This mechanism also seems to work in the PI phase.

As a concluding remark, the magnetospheric behavior in the PI phase is the elastic response of the magnetosphere acting against the sudden change in the solar wind dynamic pressure, i.e., the plastic deformation of the magnetosphere does not appear in the PI phase. In conclusion, the globally consistent magnetosphere–ionosphere coupling convection holds in the PI phase.

In the last part of this section, we note that Samsonov et al. (2010) presented another idea on the generation mechanism of the PI current system. They discussed the notion that the dynamo located on the high-latitude magnetopause behind the cusp generates the FAC in the ionosphere in the case of the PI phase (they called this current system the NBZ current system, probably because the IMF orientation used for their simulation is northward). The reason is that the time associated with the maximum FAC in the PI phase (the NBZ current in their paper) in the ionosphere, coincides with the time of maximum activity of the dynamo. However, the current flowing in the magnetopause behind the cusp is directed from the afternoon side to the morning side because the current is expressed as  $\mathbf{B} \times \nabla \cdot P/B^2$ . In this case, it seems reasonable to consider that the FAC in the ionosphere is upward/downward in the afternoon sector/morning sector. Therefore, it seems difficult to consider that this dynamo drives the PI current system which is downward/upward in the afternoon sector/morning sector.

### 3.1.2 The MI phase

When the dynamic pressure changes so gradually that the global consistency of the magnetosphere–ionosphere compound system holds, the ground magnetic variation will exhibit a simple monotonic change. However, the observation shows that the ground magnetic variations in the MI phase do not exhibit a monotonic change as shown in panels (a) and (b) of Fig. 1. The simulation does not exhibit the monotonic change either, as shown in Fig. 4. These results suggest that the global consistency is broken when the sudden change in the solar wind dynamic pressure occurs and recovers again to a new state corresponding to the new solar wind condition after the sudden dynamic pressure change, as noted in Sect. 1. In the following, we describe the physical process in the MI phase from the viewpoint of the deformation and recovery of the convection system (Fujita et al. 2003b, 2005; Fujita and Tanaka 2006). The current system which connects the magnetosphere and the ionosphere plays an essential role in the entire physical processes in the magnetosphere–ionosphere compound system (Tanaka 2007). Therefore, we will identify the current

system in the magnetosphere connecting the FAC in the ionosphere and its dynamo process.

The current system in the magnetosphere–ionosphere region in the MI phase presented by Araki (1994) is the Region 1-type FAC system (upward/downward FAC in the evening side/morning side) associated with the steady magnetosphere–ionosphere coupling convection. Following Araki (1994), the Region 1-type FAC system should be intensified because of the sudden increase in the solar wind dynamic pressure compresses the magnetosphere. Consequently, the magnetosphere–ionosphere coupling convection should also be enhanced (Fig. 3b). This concept means that a magnetosphere–ionosphere convection is established in the magnetosphere–ionosphere system immediately after the sudden change in the solar wind dynamic pressure. There are then at least two issues to be addressed for the physical model of the MI phase presented by Araki (1994). The first is the identification of the dynamo of the Region 1-type FAC system because the MI model by Araki (1994) does not discuss the dynamo. The MHD simulation (Tanaka 1995, 1999; Janhunen and Koskinen 1997; Siscoe et al. 2000) already addresses this issue. Tanaka (2007) concluded that dynamo appears in the cusp–mantle region in both the northward and southward IMF conditions. The second issue is that the Region 1-type FAC system is not constant in the MI phase as shown by the ground magnetic field changes in Fig. 1a, b. The ground magnetic variation in the MI phase initially increased then gradually weakened. Russell and Ginskey (1993) thought that this ground magnetic variation may be due to an overshoot in which the magnetosphere compressed by the sudden increase in the solar wind dynamic pressure expands once again. However, this idea has not been studied using the global MHD simulation.

The overshoot-like ground magnetic variation in the MI phase is also reproduced by the simulation as shown in Fig. 4 (Fujita et al. 2003b). Fujita et al. (2003b) revealed that the FAC variation with the Region 1-type FAC system in the ionosphere (Fig. 8) exhibits a maximum at 9.5 min and is reduced at 13.1 min. Therefore, we notice that FAC variation causes overshoot-like behavior. (Fig. 8 is a colored reproduction of Fig. 2 of Fujita et al. 2003b.) Fujita et al. (2005) also revealed an increase and decrease in the integrated ionospheric FAC intensity for the MI phase. Therefore, the mechanism of the temporal change of the FAC intensity in the ionosphere is the key issue. To address this issue, we need to investigate not only the temporal variation of the dynamo activity in the cusp–mantle region but also that of the current system connected from the dynamo in the magnetosphere to the ionosphere. (The dynamo activity can be estimated from magnitude and area of negative  $E_{\perp} \cdot J$ .) Fujita et al. (2003b) revealed that the temporal variation of the dynamo activity and that of the FAC intensity in the ionosphere are not synchronized, i.e., although the dynamo activity is activated in the period between 5.1 min and 6.0 min in Fig. 9 (the solar wind starts to compress the dynamo region in this period), the FAC intensity in Fig. 8 does not have a maximum in this period. Fujita et al. (2003b) examined the origin of the FAC in the ionosphere for the case of the MI phase using simulation results. In Fig. 10, the upward FAC flowing from the ionosphere (indicated by the blue curves) at 6.0 min indicates that it does not reach the meridian plane. (This current system is the first MI current system after Fujita et al. 2003b.) On

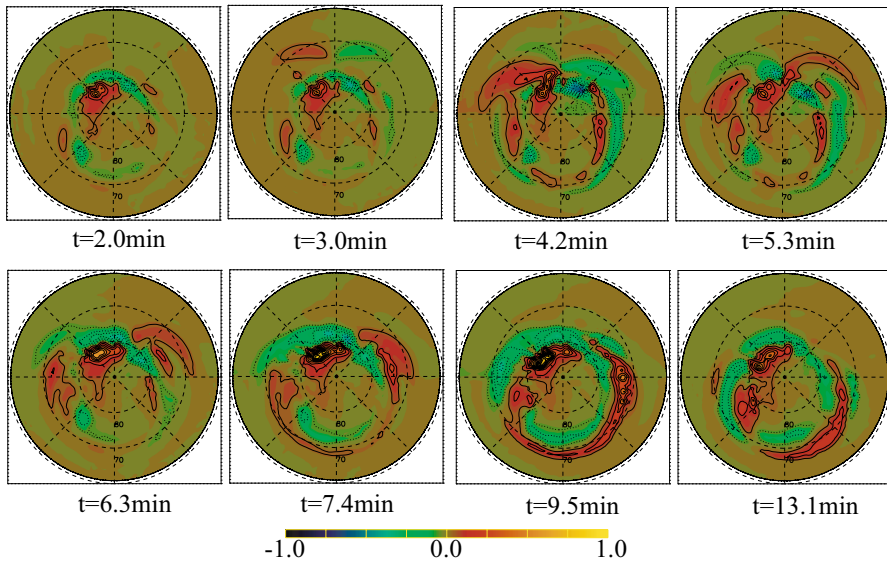


**Fig. 8** Time changes of the ionospheric FAC distribution in the whole SC interval in the northern polar region for latitudes higher than  $60^\circ$ . The top of each panel corresponds to 12 hMLT. The positive and negative FACs denote downward and upward currents, respectively. The FAC is normalized to  $5 \times 10^{-7} \text{ A/m}^2$ . This figure is a colored reproduction of Fig. 2 of Fujita et al. (2003b)

the other hand, more upward current lines from the ionosphere pass through the meridian plane. Finally, the current system becomes the steady Region 1 FAC system. Therefore, the maximum FAC in the ionosphere will appear in the latter period instead of the period of maximum activity of the dynamo at 9.1 min. We then need to determine the reason for the larger current from the dynamo in the cusp–mantle region connects to the ionosphere during this period. We describe the reason in the following part of this section.

Fujita et al. (2003b) revealed that not only the recovery of the steady Region 1 FAC system shown in Fig. 10, but also the transient plasma vortex formed in the flank of the magnetosphere in the MI phase affects the temporal variation of the FAC system. The rotation sense of this vortex is consistent with the direction of the FAC in the ionosphere in the MI phase because it exhibits anti-clockwise/clockwise circulation in the afternoon/morning side in the magnetosphere. Therefore, convection consistent with the magnetospheric flow vortex appears in the ionosphere because the FAC connects both convections. The flow vortex indicates that the field-perpendicular current generated in the dynamo region in the cusp–mantle region is converted to the FAC. Thus, the growth of the flow vortex in the magnetosphere corresponds to an increase in the FAC in the ionosphere. Consequently, the ground magnetic variation exhibits a maximum. This vortex is called the SC transient cell convection (Fujita et al. 2003b). Fujita and Tanaka (2006) explained that the inward plasma flow invoked by gradual compression of the magnetosphere flank due to the increased dynamic pressure of the solar wind and sunward convection flow in the magnetosphere generates small-scale

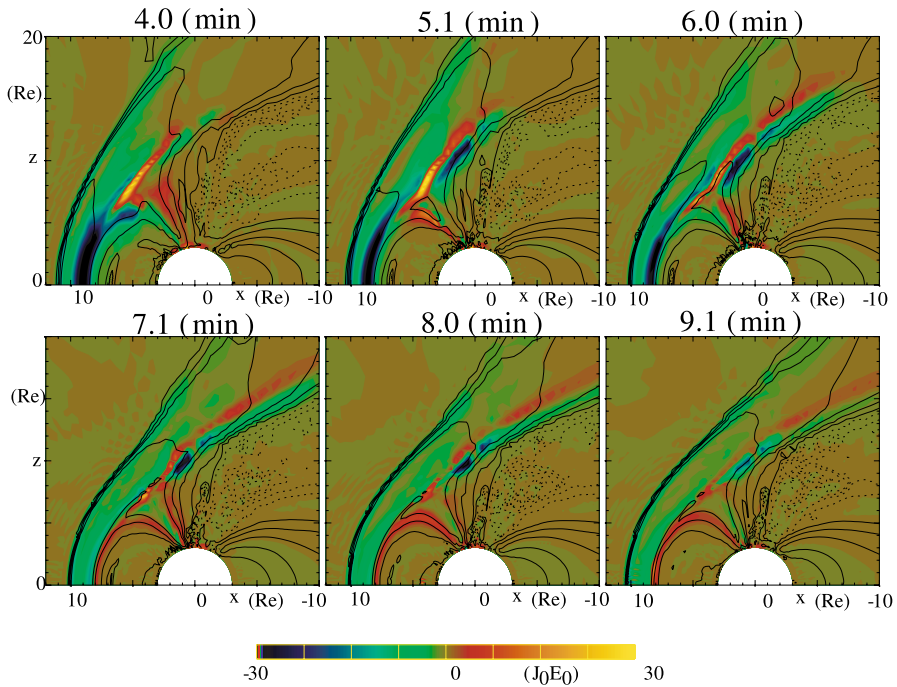


**Fig. 9** Color contours of  $J \cdot E$  normalized with  $W_0$  ( $6.6 \times 10^{-12}$  W/m<sup>3</sup>) and contour lines of  $\log p/p_0$  ( $p_0 = 46.9$  nP) for the spatial range  $-10R_e < x < 12R_e$  and  $0 < z < 20R_e$  in the day–night meridian plane. The scale for the color contour is shown at the bottom. The contour interval for  $\log p/p_0$  is 0.4. Solid and dashed contours of the pressure represent positive and negative  $\log p/p_0$ , respectively. After Fujita et al. (2003b)

plasma vortex as shown in Fig. 11. At the same time, the simulation reveals that the plasma pressure also increases in the center of this vortex (Fujita et al. 2003b; Fujita and Tanaka 2006).

The explanation of the flow vortex generation by Fujita et al. (2003b), and Fujita and Tanaka (2006) is qualitative. By applying the relationship that an increase in the plasma pressure in the magnetospheric equatorial plane yields the time derivative of the magnetic field-aligned plasma vorticity, Yu and Ridley (2009) demonstrated that the pressure gradient drives the magnetospheric flow vortex as shown in Fig. 12 for the northward IMF condition. Samsonov and Sibeck (2013) also discussed the Lorentz force associated with the electric current flowing in the pressure discontinuity in the wavefront of the FS yields a change of the field-aligned flow vortex when the IMF is northward. However, evidence of such a temporal change of the field-aligned vorticity is not clear in the southward IMF condition (Yu and Ridley 2009). Under this condition, it seems that the compression of the magnetosphere flank effectively yields a flow vortex in the magnetosphere.

Fujita et al. (2003b) explained that the enhanced pressure associated with the flow vortex in the magnetosphere also yields the secondary dynamo for the

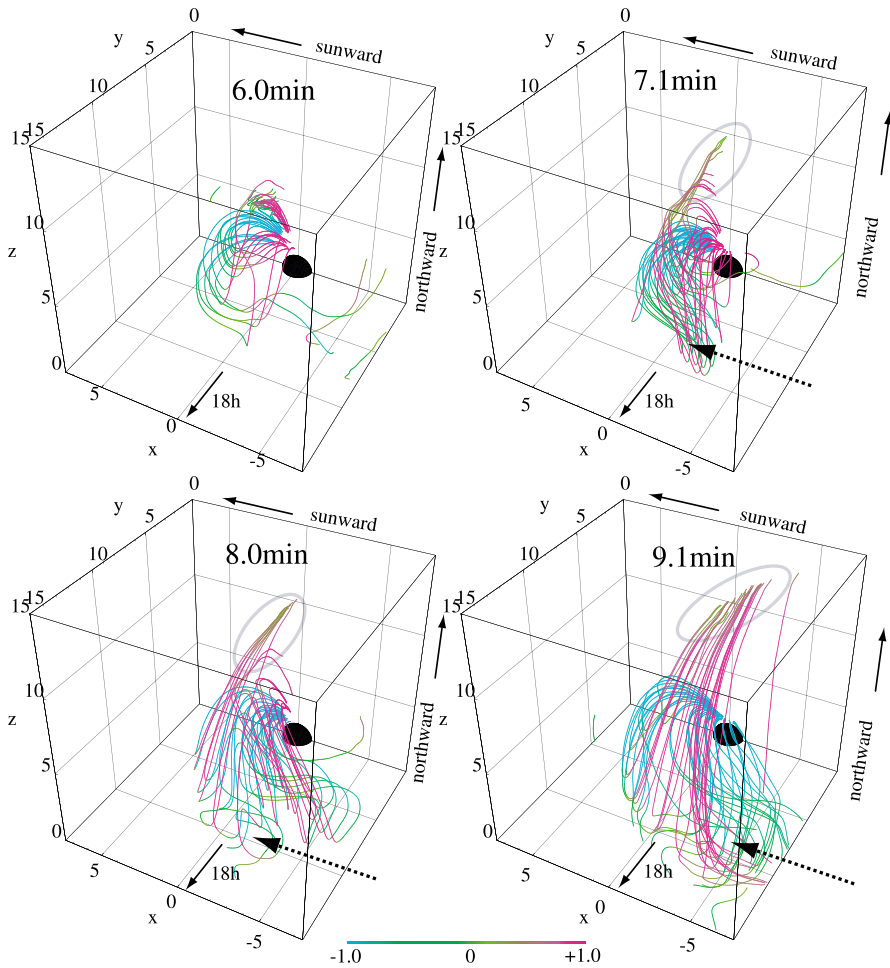


**Fig. 10** 3D pictures of the current system connected with the upward FACs at the ionospheric latitudes of  $70^{\circ}$ – $80^{\circ}$  at 6.0–9.3 min. The color of the curves denotes  $\mathbf{J} \cdot \mathbf{B} / JB = \cos \theta$ , where  $\theta$  is the angle between the electric current and the magnetic field line. The red/blue curves represent parallel/anti-parallel orientations relative to the field line ( $\cos \theta \simeq 1/-1$ ). Only the current lines with intensity larger than  $128J_0$  ( $J_0 = 0.0125 \mu\text{A}/\text{m}^2$ ) for 6.0 min and 7.1 min and  $192J_0$  for 8.0 min and 9.1 min in the ionosphere are illustrated. The current flow lines are drawn as arcs due to small-scale pressure enhancements in the region identified by broken arrows; this will be illustrated schematically in Fig. 13. Black spheres in the panels denote the Earth. Gray ellipses in the panels for 7.1, 8.0, and 9.1 min indicate the areas through which the upward FAC from the ionosphere in the afternoon side (indicated by blue curves) passes over the noon–midnight meridian. After Fujita et al. (2003a)

FAC system in the MI phase as schematically shown in Fig. 13. This dynamo was also confirmed by Yu and Ridley (2009) and Samsonov et al. (2010). Therefore, we conclude that the SC transient cell convection yields an overshoot-like variation of the ground magnetic variations. Figure 13 is an alternative image of Fig. 2b which explains the current system in the MI phase. The SC transient cell

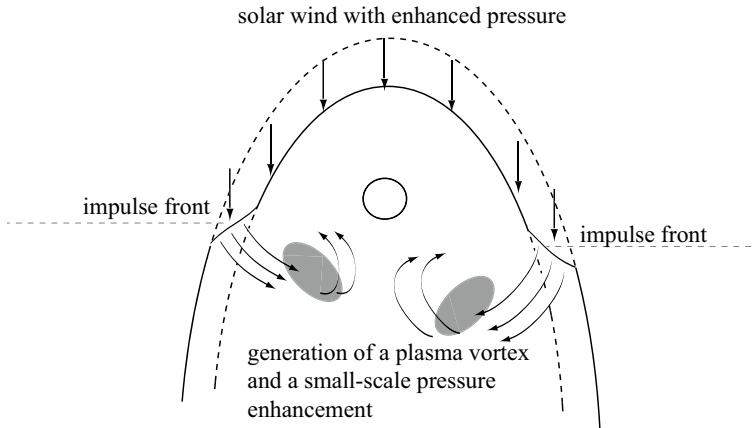
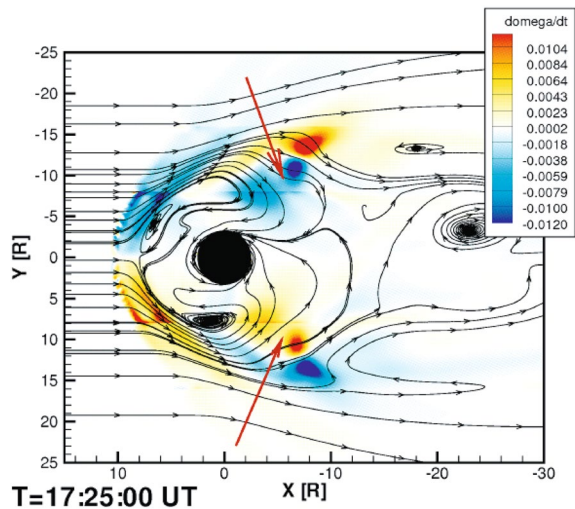


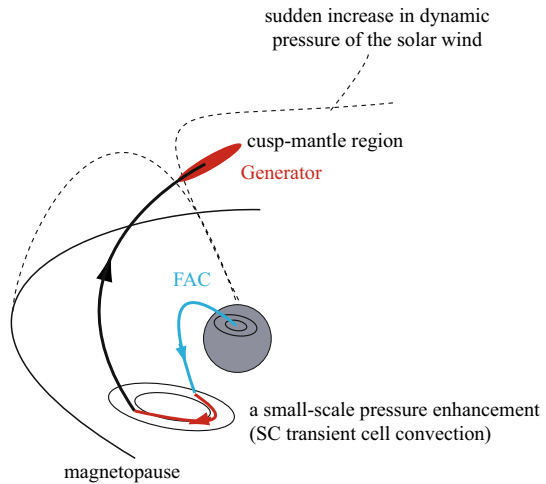
**Fig. 11** A schematic illustration of plasma disturbances in the magnetospheric equatorial plane for the MI phase. Gradual compression of the magnetosphere flank due to a solar wind impulse invokes a transient plasma vortex (a convection cell) and a small-scale pressure enhancement in the magnetosphere. After Fujita and Tanaka (2006)

**Fig. 12** The black streamlines represent plasma convection in the equatorial plane, and the color contour is  $d\Omega_{\parallel}/dt$  where  $\Omega_{\parallel}$  indicates that the flow vorticity is parallel to the magnetic field in the northward IMF condition in the MI phase. The unit of  $d\Omega_{\parallel}/dt$  is  $10^{-3}/s$ . Positive/negative  $d\Omega_{\parallel}/dt$  in the evening/morning side magnetosphere indicates an increase in the anti-clockwise/clockwise vortex. After Yu and Ridley (2009)



convection seems to “generate” the FAC because this flow vortex is associated with the dynamo (Yu and Ridley 2009; Samsonov et al. 2010). However, because of the relation of  $\nabla_{\perp} \cdot \mathbf{J}_{\perp} + \nabla_{\parallel} \cdot \mathbf{J}_{\parallel} = 0$ , the FAC should be “converted” from a perpendicular current. Therefore, it is important to investigate the current system in the magnetosphere–ionosphere region as shown in Figs. 10 and 13. The SC transient cell has also been reported on based on simulations (Kim et al. 2009; Sun et al. 2015). This has also been confirmed by recent observation (Samsonov et al. 2014).

**Fig. 13** A schematic illustration of the current system in the magnetosphere–ionosphere region in the MI phase. The flow vortex of the SC transient cell convection in the magnetosphere converts the field-perpendicular current (black) to the FAC (blue). The small-scale pressure enhancement invoked by the SC transient cell convection yields the secondary dynamo shown by the red curve in the SC transient cell convection. After Fujita and Tanaka (2006)



Here, let us interpret the MI process from the viewpoint of the magnetosphere–ionosphere compound system after Fujita et al. (2005), Fujita and Tanaka (2006). The magnetosphere–ionosphere compound system defines a unique state of the magnetosphere and the ionosphere corresponding to the constant solar wind condition. Thus, the SC process can be interpreted as the state transition of the compound system by the sudden change of the solar wind dynamic pressure. As noted above, when the enhanced dynamic pressure of the solar wind compresses the dynamo region of the Region 1-type FAC system (the cusp–mantle region), the FAC of the MI phase in the ionosphere (upward/downward in the afternoon/morning sector) is not maximized. This result represents a violation of the global consistency of the magnetosphere–ionosphere compound system. The SC transient cell convection plays an essential role in the regeneration of global consistency, i.e., the steady magnetosphere–ionosphere coupling convection. The SC transient cell convection invokes the upward/downward FACs in the afternoon/morning sector of the magnetosphere. This FAC corresponds to the Region 1-type FAC system. When the front of the sudden enhancement of the solar wind dynamic pressure compresses the magnetopause, the pressure gradient in front of the compressional wave drives the flow vortex. Thus, the SC transient cell convection starts to grow. When the pressure gradient in the magnetosphere is reduced behind the compressional wave passing to the tail region, the transient cell takes over the large-scale magnetospheric convection corresponding to the normal Region 1 FAC system. Then, the ground magnetic variation of the MI phase becomes constant. The steady convection in the magnetosphere–ionosphere compound system is completely regenerated. As noted above, the FAC intensity in the ionosphere is related to the generation and attenuation of the SC transient cell convection, and not to the dynamo activity in the cusp–mantle region. Thus, the overshoot-like variation of the ground magnetic field and the SC transient cell convection connect to each other. Namely, the overshoot like variation is a proxy for the state transition of the magnetosphere–ionosphere compound system.

In summary, the global physical process in the MI phase is the transition of the magnetosphere–ionosphere state to a new steady state suitable for a new solar wind condition after the sudden change in the solar wind dynamic pressure (Fujita et al. 2005). The SC transient cell convection plays a crucial role in the state transition. Compared with plasma disturbances in the PI phase, those in the MI phase exhibit a slower behavior. Thus, inertia does not play a role in the MI phase, unlike the PI phase. The magnetospheric current is the diamagnetic current which is driven by the force balance between the plasma pressure and the magnetic tension force (the Lorentz force) (Fujita et al. 2003a).

### 3.2 The simulation study of the MHD waves associated with the SC

When the sudden change in the solar wind dynamic pressure arrives at the dayside magnetopause, a fast magnetosonic wave propagates into the magnetosphere in the PI phase. Then, the coupling resonance theory (Tamao 1965) predicts that a standing Alfvén wave is excited due to the coupling with the fast magnetosonic wave in the magnetosphere. To reproduce the field-aligned propagation of the Alfvén wave in the simulation, we need to use a particular grid system with reference to the magnetic field lines. (If the grid system is not along the field line, the field-aligned difference in the simulation has to transmit a signal of the Alfvén wave on one field line to the other field line.) No global MHD simulation employs such a coordinate system. Therefore, we explain the results of the recent modeling study based separately on the MHD wave simulation codes. Note that the MHD wave simulation treats only propagation of a linear MHD wave on the background stationary magnetic field, say, the dipole field.

The MHD waves can be excited in the magnetosphere by the sudden change in the solar wind dynamic pressure. Recent numerical studies on this phenomenon have investigated the wave generation property of the coupled MHD wave of the Alfvén wave and the fast magnetosonic wave in the realistic magnetosphere. In these studies, sudden intensification of the east–west component of the electric field on the magnetopause mimics sudden compression of the magnetopause by an increase in the solar wind dynamic pressure (Lee and Lysak 1989).

Although the linear impulse response of a simplified magnetosphere was previously investigated (e.g., Allan and Knox 1979), the realistic magnetosphere model has been employed in simulation since the late 1980s. Lee and Lysak (1989) performed simulation studies on the excitation of the MHD waves by the sudden increase in the solar wind dynamic pressure in the magnetosphere with a dipole magnetic field. They demonstrated that the sudden increase in the dynamic pressure excites both the global compressional mode (the fast magnetosonic wave) in the magnetospheric cavity and the field-line resonance mode (the Alfvén wave bouncing between ionospheres in both hemispheres). The latter modes are excited by a resonance coupling mechanism proposed by Tamao (1965). Later, Lee (1996) showed that an enhancement in Alfvén speed in the outer boundary of the plasmasphere controls the behavior of the excited global mode. Finally, Lee and Kim (1999) revealed that the MHD waves are partly trapped in the plasmasphere with sufficient energy to



escape across the plasmapause to become damped waves. They named this cavity-like oscillation as the plasmaspheric virtual resonance. These studies attempted to reproduce the ULF waves, Psc, associated with the SC (Wilson and Sugiura 1961; Saito 1969) which exhibits a damping waveform with a period of about 100 s.

The Psc study with the global MHD simulation has not been performed so much. Claudepierre et al. (2009) reported on the magnetospheric resonant oscillation caused by a periodic fluctuation of the solar wind dynamic pressure in the dayside magnetosphere. This oscillation is not the Psc, but this study suggested the existence of the global magnetospheric resonant mode which can be excited by the sudden change of the solar wind dynamic pressure. The simulation study by Yu and Ridley (2011) also discussed that the sudden change of the dynamic pressure in the solar wind generates transient plasma disturbances that are trapped in the dayside magnetosphere between the magnetopause and the inner magnetosphere. Since this disturbance is a transient one accompanying the SC, this phenomenon may be the Psc. Note that this disturbance belongs to the compressional mode (the global mode, the fast magnetosonic wave). They did not show the disturbances associated with the toroidal mode (the field-line resonance mode, the Alfvén). Samsonov et al. (2011) also investigated the frequencies of the magnetospheric disturbances observed by satellites and those calculated using MHD simulations. They revealed that both disturbances have common frequencies for the poloidal mode. However, they concluded that the toroidal mode appears in the satellite observations but does not appear in the simulation results. This fact is probably due to the deficiency of the global MHD simulation in that it cannot reproduce the Alfvén wave exactly as previously noted. The field-line resonance mode (the toroidal mode) stimulated by the SC is observed on the ground (Yumoto et al. 1997). Therefore, the present global MHD simulation does not reproduce this standing mode. Finally, we note that Kubota et al. (2015) reported on the reproduction of the Psc in the horizontal magnetic variations on the ground reproduced by the global MHD simulation of the intensive SC. They insisted that the Psc is associated with only the high-intensity SC. Note that they did not discuss whether the standing Alfvén wave is reproduced or not in the simulation.

The Pi2 pulsation is the pulsation excited by the sudden change of the plasma sheet (Keiling and Takahashi 2011). Thus, the Psc can be regarded as a counterpart of the Pi2 pulsation in the dayside magnetosphere. It is well-known that the Pi2 pulsation is almost always associated with the substorm onset (Keiling and Takahashi 2011; Zhang et al. 2010). Therefore, it is interesting to investigate the occurrence probability of the Psc. The simulation study suggests that the Psc is excited during the massive increase of the solar wind dynamic pressure (Kubota et al. 2015). However, there is no statistical study on the occurrence of the Psc. Systematic observational studies on the condition of the Psc excitation are required.

#### 4 Other topics of the SC in the global MHD simulation

The present paper summarizes SC studies based on global MHD simulations from the viewpoint of break and recovery of the global consistency of the magnetosphere–ionosphere compound system. Therefore, the previous section did not

describe the recent works on the unknown behaviors of the plasmas revealed by the simulations, and those related to the elucidation of the observed phenomena reproduced by the simulations. These simulation studies were mainly performed to elucidate the cause-to-effect relations of the phenomena associated with the SC. In the last section of this paper, we will address these topics.

#### 4.1 SCs in extreme solar wind conditions

There is significant merit in the application of computer simulation to simulate phenomena under extraordinary conditions. We can obtain new information about the characteristics of the magnetosphere–ionosphere system by investigating the response of the magnetosphere to the FS and the TD under abnormal solar wind conditions. Furthermore, for this purpose, it is necessary to develop a robust code. Such improvement of simulation code enables us to investigate extremely severe SC events. The study of the extremely severe SC is also meaningful to the space weather because the intensified electric field associated with severe SC significantly accelerates high-energy particles in the radiation belt (Wygant et al. 1994) and because such a rapidly varying ground magnetic field generates severe geomagnetic induced currents (Kappenman 2003).

Ridley et al. (2006) calculated the response of the magnetosphere–ionosphere system for coronal mass ejection (CME) corresponding to the Carrington storm (Tsurutani et al. 2003). Their simulation employed the solar wind CME parameters upstream of the magnetosphere provided by the MHD simulation of the solar wind (Manchester et al. 2006), as a driver of the magnetosphere simulation. As a result, Ridley et al. (2006) reported a bifurcation of the bow shock. The bow shock in the Earthside bounces at the inner boundary of the Earth and becomes unified with the original bow shock. The ionospheric FAC distribution and the potential distribution associated with such a severe interplanetary shock are essentially the same as those of the SC caused by the TD in the typical solar wind condition with a density increase (Fujita et al. 2003a, b).

Kubota et al. (2015) also presented results for severe SCs using several sets of severe solar wind interplanetary shocks based on the improved simulation code (Tanaka 2015). They employed the shock condition (the Rankine–Hugoniot relation) which represents the interplanetary shock in the solar wind as demonstrated by Guo et al. (2005). As a result, they revealed that the intensified solar wind shock yields an SC with sharp variations of the ground magnetic fields. Also, the Psc will accompany the extremely large SC caused by intensified changes in the solar wind dynamic pressure as noted in Sect. 3.2.

Yu and Ridley (2011) investigated the SC for low-Mach number solar wind, but still super-Alfvénic. The low-Mach number solar wind is implemented in the simulation by utilizing the enhanced Alfvén speed due to reduced solar wind density or intensified IMF. The SC in the low-Mach solar wind does not show a clear two-step response (PI and MI). They explained that the single response is attributed to prolonged PI phase and reduced variations of the MI phase. They also discussed that

energy transported into the magnetosphere is reduced in the case of the low-Mach number solar wind.

#### 4.2 Generation and propagation of MHD disturbances at the SC

The interplanetary discontinuities in the solar wind driving the SC are the TD and the FS. When this discontinuity impinges on the bow shock, the secondary discontinuities propagate in the magnetosheath and are reflected in the solar wind. Also, the forwarding discontinuity in the magnetosheath induces another discontinuity into the magnetosphere and back to the magnetosheath at the magnetopause.

Samsonov et al. (2007) discussed such interaction of the FS in the solar wind and the magnetosphere (the bow shock, the magnetosheath, the magnetopause, and the magnetosphere). In particular, they confirmed that when the FS impinges on the dayside bow shock, it starts to move toward the magnetosheath. Similarly, when the FS that is propagated into the magnetosheath collides with the magnetopause, the magnetopause also begins to move towards the Earth. Next, the FS which transmits to the dayside magnetosphere is reflected in the inner boundary of the numerical model. Finally, the FS returns to the magnetopause. The magnetopause then ceases to move, and the reflected FS transmitted to the magnetosheath from the magnetosphere arrives at the bow shock, and the bow shock stops. Yu and Ridley (2011) also investigated the bouncing of the discontinuity between the bow shock and the numerical inner boundary of the magnetosphere. (They called the discontinuity the MHD wave.) The bouncing period is approximately 2 min. Thus, this bouncing wave may be the Psc (Wilson and Sugiura 1961; Saito 1969). Samsonov and Sibeck (2013) discussed the importance of the discontinuity for the generation of the flow vortex in the magnetosphere in the MI phase because the Lorentz force is associated with the enhanced current in the wavefront of the discontinuity.

#### 4.3 The negative SC

When a sudden decrease in the solar wind dynamic pressure arrives in the magnetosphere, a phenomenon called negative SC occurs. Negative SC was first studied by Araki and Nagano (1988). This phenomenon seems to be a mirror image of positive SC. The global MHD simulation confirms this mirror image relation (Fujita et al. 2004). Recently, ionospheric flow generated during the negative SC has been reported to show morning–evening asymmetry using the superDARN radar observation (Hori et al. 2012). A recent simulation study (Fujita et al. 2012) explains the superDARN result.

On the other hand, the simulation study of the negative SC shows an interesting temporal variation of the ionospheric FAC distribution from the viewpoint of the magnetosphere–ionosphere compound system (Fujita et al. 2012). In the simulation result on the negative SC, the daytime magnetosphere expands outward and then rebound several times during the negative SC. In the daytime ionosphere, upward/downward FAC appears in the afternoon/morning side in the PI phase. This current pattern is the reverse sense of the usual PI current pattern of the positive SC.

This PI current system of the negative SC has the FAC in the ionosphere with the same sense of the Region 1-type FAC system. These patterns of the FAC move to the evening side. Then the downward/upward FAC appears on the low latitude side of the PI current system in the afternoon/morning. This current system should be called the MI variation of the negative SC. The FAC of the current system has the same character as the Region 2 FAC system (downward in the afternoon side, upward in the afternoon) (Iijima and Potemra 1976). In the steady state, the magnetosphere–ionosphere compound system has the Region 1 FAC system in the higher latitude side and the Region 2 FAC system in the equatorial side in the polar ionosphere. As for the positive SC, the transient MI current system gradually changes to the steady Region 1 FAC system. However, because the current direction of the MI current system is the same as that of the Region 2 FAC system for the negative SC, there should be a consequent phase in which the Region 1-type FAC appears. Therefore, the number of phases is different between the positive SC and the negative SC. The SC transient cell convection of the negative SC has three stages, a clockwise vortex, then a counterclockwise vortex, and finally a clockwise vortex in the afternoon, in the magnetospheric equatorial plane. The behavior of the SC transient cell convection is a characteristic feature of the state transition for the negative SC, which is different from that for the positive SC. Namely, this result does not support the mirror image idea of the positive SC and the negative SC.

#### 4.4 Other topics

Since the magnetosphere–ionosphere region is in contact with the thermosphere, the magnetospheric disturbances would affect the neutral atmosphere in the thermosphere. Zou et al. (2017) and Ozturk et al. (2018) investigated the thermospheric response to the SC by comparing observational facts and simulation results. The intensified FAC in the SC period gives excess energy to the thermosphere. These two publications examined this issue using the combined numerical model of BATS-R-US (the MHD model), CRCM (the Ring current model), and RIM (the ionosphere model). Zou et al. (2017) discussed plasma behavior under the ionospheric electric field induced by the SC in the F region. These results are consistent with the incoherent scatter radar observations of the ionospheric plasmas. Ozturk et al. (2018) revealed that the FAC associated with the ionospheric electric field induced by the SC significantly transfers the energy to the plasmas and neutral particles in the high-latitude ionosphere by the frictional heating. However, they indicated that the simulation results exhibited a smaller magnitude compared to the observed results. However, the simulation study of the magnetosphere–ionosphere–thermosphere was only recently commenced. The fully coupled code of the magnetosphere–ionosphere system and the thermosphere (Ridley et al. 2003) should be utilized in this study in the future.

An argument has been presented on the SC-triggered substorm. Keika et al. (2009) reported that the SC triggered the substorm expansion from the analysis of the THEMIS data. On the other hand, Meurant et al. (2005) discussed that the SC does not trigger substorm expansion. Also, Zhou and Tsurutani (2001) reported that

the substorm is triggered by the SC when the magnetotail plasma state is ready for the onset (pre-conditioning). There are no papers on this issue based on simulation studies. Also, the auroras associated with the SC (the shock aurora) (Zhou et al. 2003) remains as one of the future issues which have not been treated by the global MHD simulations.

The wavefront of the interplanetary shock is not always perpendicular to the Sun–Earth axis. Guo et al. (2005) treated the SC as a shock whose wavefront is oblique to the Sun–Earth axis by using the Chinese MHD code proposed by Hu et al. (2005). The shock propagates along the Sun–Earth axis. They presented the dawn–dusk asymmetry of the deformation of the magnetosphere. Later, Samsonov et al. (2015) and Selvakumaran et al. (2017) also investigated the magnetosphere–ionosphere response to the oblique interplanetary shock. Samsonov et al. (2015) employed the oblique shock that impinges on the dusk side of the magnetosphere. They revealed that the dusk side magnetosphere is compressed, but the dawn side magnetosphere expands due to the solar wind shock.

## 5 Conclusion

This report describes the SC process from the viewpoint of the state transition of the magnetosphere–ionosphere compound system. This viewpoint encompasses a new examination of SC; individual disturbances (elementary processes) in various regions from the magnetosphere to the ground compete and settling to a new steady state of the magnetosphere–ionosphere compound system. This idea originated from realistic global MHD simulations. The main results of this investigation are as follows:

The simulation validates the model compiled from observations and relevant theoretical considerations on the PI. The PI phase is characterized by an elastic response of the magnetosphere–ionosphere system. The transient current system in the magnetosphere–ionosphere region is excited as a linear response of the magnetosphere.

The MI phase is the state transition of the magnetosphere–ionosphere compound system due to the sudden change of the solar wind dynamic pressure.

The overshoot-like variation of the ground magnetic variation is a proxy of the state transition of the magnetosphere–ionosphere compound system during the SC period. The SC transient cell convection and the FAC compete for each other and gradually settle into the globally consistent state. During this process, enhanced SC transient cell convection leads to the enhanced FAC in the ionosphere. The enhanced FAC causes an enhanced ionospheric potential. A gradual reduction in the intensity of the SC transient cell convection and the ionospheric FAC causes a reduction of the ground magnetic variation. Thus, the overshoot-like variation appears.

Furthermore, the following simulation studies were discussed in this paper.

It is important to treat the SC in the extreme conditions of the solar wind because such event may give us new findings of the magnetosphere–ionosphere system as well as the extreme events may have important consequences to the lower atmosphere, and to human activities. There are two simulation studies regarding the SCs in the extremely severe solar wind condition and those in the low-Mach solar wind. These simulation studies yield the results different from those of the SCs in the normal solar wind condition. These studies should be promoted in the future because they are not only expected to be applied to space weather but also to promote a robust simulation code.

The simulated SC associates the MHD disturbances bouncing between the inner boundary and the magnetopause in the dayside magnetosphere. This disturbance seems to be the Psc in the dayside magnetosphere. We need observational confirmation of this event.

It is important to study the relation between the substorm and the SC, but there is no simulation work about this topic.

**Acknowledgements** I would like to thank T. Araki of Kyoto Univ., T. Kikuchi of Nagoya Univ., D.-H. Lee of Kyung Hee Univ., and R. Kataoka of Nat. Inst. Polar Res. I am also thankful to referees for constructive comments. This work was supported by JSPS KAKENHI Grant Numbers JP17K05671 and JP15H05815 (PSTEP). This work is one of the outcomes of the NIPR project KP301. The computations for this study were performed using supercomputers installed at the Polar Data Center of NIPR and “One Space Net” of NICT (National Institute of Information and Communication Technology). The production of this paper was supported by a NIPR publication subsidy. We would like to thank Editage (<http://www.editage.jp>) for English language editing.

## References

- W. Allan, K.B. Knox, A dipole field model for axisymmetric Alfvén waves with finite ionosphere conductivities. *Planet. Space Sci.* **27**, 79–85 (1979)
- T. Araki, Global structure of geomagnetic sudden commencements. *Planet. Space Sci.* **25**, 373–384 (1977)
- T. Araki, A physical model of the geomagnetic sudden commencement, in *Solar Wind Sources of Magnetospheric Ultra-Low-Frequency Waves*, ed. by M.J. Engebretson, K. Takahashi, M. Scholer (American Geophysical Union, Washington, DC, 1994), pp. 183–200
- T. Araki, H. Nagano, Geomagnetic response to sudden expansions of the magnetosphere. *J. Geophys. Res.* **93**, 3983–3988 (1988)
- W. Baumjohann, R.A. Treumann, *Basic Space Plasma Physics* (Imperial College Press, London, 1997)
- P.J. Chi, C.T. Russell, Travel-time magnetoseismology: magnetospheric sounding by timing the tremors in space. *Geophys. Res. Lett.* **32**, L18108 (2005). <https://doi.org/10.1029/2005GL023441>
- P.J. Chi, C.T. Russell, J. Raeder, E. Zesta, K. Yumoto, H. Kawano, K. Kitamura, S.M. Petrinec, V. Angelopoulos, G. Le, M.B. Moldwin, Propagation of the preliminary reverse impulse of sudden commencements to low latitudes. *J. Geophys. Res.* **106**, 18857–18864 (2001)
- P.J. Chi, C.T. Russell, J. Raeder, E. Zesta, K. Yumoto, H. Kawano, K. Kitamura, S.M. Petrinec, V. Angelopoulos, G. Le, M.B. Moldwin, Reply to comment by T. Kikuchi and T. Araki on “Propagation of the preliminary reverse impulse of sudden commencements to low latitudes”. *J. Geophys. Res.* **107**(A12), 1474 (2002). <https://doi.org/10.1029/2002JA009369>
- S.G. Claudepierre, M. Wiltberger, S.R. Elkington, W. Lotko, M.K. Hudson, Magnetospheric cavity modes driven by solar wind dynamic pressure fluctuations. *Geophys. Res. Lett.* **36**, L13101 (2009). <https://doi.org/10.1029/2009GL039045>
- J.W. Dungey, Interplanetary magnetic field and the auroral zones. *Phys. Rev. Lett.* **6**, 47 (1961)

- M.J. Engebretson, D.L. Murr, W.J. Hughes, H. Lühr, T. Moretto, J.L. Posch, A.T. Weatherwax, T.J. Rosenberg, C.G. MacLennan, L.J. Lanzerotti, F. Marcucci, S. Dennis, G. Burns, J. Bitterly, M. Bitterly, A multipoint determination of the propagation velocity of a sudden commencement across the polar ionosphere. *J. Geophys. Res.* **104**, 22433–22451 (1999)
- J.A. Fedder, J.G. Lyon, The solar wind–magnetosphere–ionosphere current–voltage relationship. *Geophys. Res. Lett.* **14**(8), 880–883 (1987). <https://doi.org/10.1029/GL014i008p00880>
- J.A. Fejer, Atmospheric tides and associated magnetic effects. *Rev. Geophys.* **2**(2), 275–309 (1964). <https://doi.org/10.1029/RG002i002p00275>
- E. Friis-Christensen, Y. Kamide, A.D. Richmond, S. Matsushita, Interplanetary magnetic field control of high-latitude electric fields and currents determined from Greenland Magnetometer Data. *J. Geophys. Res.* **90**(A2), 1325–1338 (1985). <https://doi.org/10.1029/JA090iA02p01325>
- S. Fujita, T. Tanaka, Magnetospheric Plasma Processes During a Sudden Commencement Revealed from a Global MHD Simulation. in: *Magnetospheric ULF Waves: Synthesis and New Directions* ed. by K. Takahashi, P. J. Chi, R. E. Denton, R. L. Lysak. (2006). <https://doi.org/10.1029/169GM05>
- S. Fujita, T. Tanaka, T. Kikuchi, K. Fujimoto, K. Hosokawa, M. Itonaga, A numerical simulation of the geomagnetic sudden commencement: 1. Generation of the field-aligned current associated with the preliminary impulse. *J. Geophys. Res.* **108**(A12), 1416 (2003a). <https://doi.org/10.1029/2002J A009407>
- S. Fujita, T. Tanaka, T. Kikuchi, K. Fujimoto, M. Itonaga, A numerical simulation of the geomagnetic sudden commencement: 2. Plasma processes in the main impulse. *J. Geophys. Res.* **108**(A12), 1417 (2003b). <https://doi.org/10.1029/2002JA009763>
- S. Fujita, T. Tanaka, T. Kikuchi, S. Tsunomura, A numerical simulation of a negative sudden impulse. *Earth Planets Space* **56**, 463–472 (2004)
- S. Fujita, T. Tanaka, T. Motoba, A numerical simulation of the geomagnetic sudden commencement: 3. A sudden commencement in the magnetosphere-ionosphere compound system. *J. Geophys. Res.* **110**, A11203 (2005). <https://doi.org/10.1029/2005JA011055>
- S. Fujita, H. Yamagishi, K.T. Murata, M. Den, T. Tanaka, A numerical simulation of a negative solar wind impulse: revisited. *J. Geophys. Res.* **117**, A09219 (2012). <https://doi.org/10.1029/2012JA017526>
- K.-H. Glassmeier, M. Hönisch, J. Untiedt, Ground-based and satellite observations of traveling magnetospheric convection twin vortices. *J. Geophys. Res.* **94**, 2520–2528 (1989)
- T.I. Gombosi, K.G. Powell, D.L. De Zeeuw, Axisymmetric modeling of cometary mass loading on an adaptively refined grid: MHD results. *J. Geophys. Res.* **99**, 21525–21539 (1994)
- X.-C. Guo, Y.-Q. Hu, C. Wang, Earth's magnetosphere impinged by interplanetary shocks of different orientations. *Chin. Phys. Lett.* **22**, 3221–3224 (2005). <https://doi.org/10.1088/0256-307X/22/12/067>
- T. Hori, A. Shinbori, N. Nishitani, T. Kikuchi, S. Fujita, T. Nagatsuma, O. Troshichev, K. Yumoto, A. Moiseyev, K. Seki, Evolution of negative SI-induced ionospheric flows observed by SuperDARN King Salmon HF radar. *J. Geophys. Res.* **117**, A12223 (2012). <https://doi.org/10.1029/2012JA018093>
- Y.-Q. Hu, X.-C. Guo, G.-Q. Li, C. Wang, Z.-H. Huang, Oscillation of quasi-steady earth's magnetosphere. *Chin. Phys. Lett.* **22**, 2723–2726 (2005)
- W.J. Hughes, The magnetopause, magnetotail, and magnetic reconnection, in *Introduction to Space Physics*, ed. by M. Kivelson, C.T. Russell (Cambridge University Press, Cambridge, 1995), pp. 227–287
- T. Iijima, T.A. Potemra, The amplitude distribution of field-aligned currents at northern high latitudes observed by Triad. *J. Geophys. Res.* **81**(13), 2165–2174 (1976). <https://doi.org/10.1029/JA081i013p02165>
- P. Janhunen, H.E.J. Koskinen, The closure of region-1 field-aligned current in MHD simulation. *Geophys. Res. Lett.* **24**, 1419–1422 (1997)
- J.A. Joselyn, B.T. Tsurutani, Geomagnetic sudden impulses and storm sudden commencements. A note on terminology. *EOS* **47**, 1808–1809 (1990)
- J.G. Kappenman, Storm sudden commencement events and the associated geomagnetically induced current risks to ground-based systems at low-latitude and midlatitude locations. *Space Weather* **1**(3), 1016 (2003). <https://doi.org/10.1029/2003SW000009>
- R. Kataoka, H. Fukunishi, S. Fujita, T. Tanaka, M. Itonaga, Transient response of the Earth's magnetosphere to a localized density pulse in the solar wind: simulation of traveling convection vortices. *J. Geophys. Res.* **109**, A03204 (2004). <https://doi.org/10.1029/2003JA010287>
- K. Keika, R. Nakamura, W. Baumjohann, V. Angelopoulos, P.J. Chi, K.H. Glassmeier, M. Fillingim, W. Magnes, H.U. Auster, K.H. Fornacon, G.D. Reeves, K. Yumoto, E.A. Lucek, C.M. Carr, I.

- Dandouras, Substorm expansion triggered by a sudden impulse front propagating from the dayside magnetopause. *J. Geophys. Res.* **114**, A00C24 (2009). <https://doi.org/10.1029/2008JA013445>
- A. Keiling, K. Takahashi, Review of Pi2 Models. *Space Sci Rev.* **161**, 63–148 (2011). <https://doi.org/10.1007/s11214-011-9818-4>
- K.A. Keller, M. Hesse, M. Kuznetsova, L. Rastätter, T. Moretto, T.I. Gombosi, D.L. DeZeeuw, Global MHD modeling of the impact of a solar wind pressure change. *J. Geophys. Res.* **107**(A7) (2002). <https://doi.org/10.1029/2001JA000060>
- T. Kikuchi, K.K. Hashimoto, I. Tomizawa, Y. Ebihara, Y. Nishimura, T. Araki, A. Shinbori, B. Veenadhari, T. Tanaka, T. Nagatsuma, Response of the incompressible ionosphere to the compression of the magnetosphere during the geomagnetic sudden commencements. *J. Geophys. Res. Space Phys.* **121** (2016). <https://doi.org/10.1002/2015JA022166>
- T. Kikuchi, T. Araki, Transient response of uniform ionosphere and preliminary reverse impulse of geomagnetic storm sudden commencement. *J. Atmos. Terr. Phys.* **41**, 917–925 (1979a)
- T. Kikuchi, T. Araki, Horizontal transmission of the polar electric field to the equator. *J. Atmos. Terr. Phys.* **41**, 927–936 (1979b)
- T. Kikuchi, T. Araki, H. Maeda, K. Maekawa, Transmission of polar electric fields to the equator. *Nature* **273**, 650 (1978)
- K.-H. Kim, K.S. Park, T. Ogino, D.-H. Lee, S.-K. Sung, Y.-S. Kwak, Global MHD simulation of the geomagnetic sudden commencement on 21 October 1999. *J. Geophys. Res.* **114**, A08212 (2009). <https://doi.org/10.1029/2009JA014109>
- M.G. Kivelson, D.J. Southwood, Ionospheric travelling vortex generation by solar wind buffeting of the magnetosphere. *J. Geophys. Res.* **96**, 1661–1667 (1991)
- Y.R. Kubota, M. Kataoka, T. Den, T. Nagatsuma, Tanaka, S. Fujita, Global MHD simulation of magnetospheric response of preliminary impulse to large and sudden enhancement of the solar wind dynamic pressure, *Earth. Planets Space* **67**, 94 (2015). <https://doi.org/10.1186/s40623-015-0270-7>
- D.-H. Lee, Dynamics of MHD wave propagation in the low-latitude magnetosphere. *J. Geophys. Res.* **101**, 15371–15386 (1996)
- D.-H. Lee, K. Kim, Compressional MHD waves in the magnetosphere: a new approach. *J. Geophys. Res.* **104**, 12379–12385 (1999)
- D.-H. Lee, R.L. Lysak, Magnetospheric ULF wave coupling in the dipole model: the impulsive excitation. *J. Geophys. Res.* **94**, 17097–17103 (1989)
- K. Maezawa, Magnetospheric convection induced by the positive and negative Z components of the interplanetary magnetic field: quantitative analysis using polar cap magnetic records. *J. Geophys. Res.* **81**(13), 2289–2303 (1976)
- W.B. Manchester IV, A. Ridley, T. Gombosi, D. De Zeeuw, Modeling the Sun–Earth propagation of a very fast CME. *Adv. Space Res.* **38**, 253–262 (2006)
- M. Meurant, J.-C. Gérard, C. Blockx, V. Coumans, B. Hubert, M. Connors, L.R. Lyons, E. Donovan, Comparison of intense nightside shock-induced precipitation and substorm activity. *J. Geophys. Res.* **110**, A07228 (2005). <https://doi.org/10.1029/2004JA010916>
- T. Moretto, A.J. Ridley, M.J. Engebretson, O. Rasmussen, High-latitude ionospheric response to a sudden impulse event during northward IMF conditions. *J. Geophys. Res.* **105**, 2521–2531 (2000)
- T. Nagata, S. Kokubun, A particular geomagnetic daily variation ( $S_p^p$ ) in the polar regions on geomagnetically quiet days. *Nature* **195**, 555–557 (1962). <https://doi.org/10.1038/195555a0>. (11 August 1962)
- A. Nishida, Ionospheric screening effect and storm sudden commencement. *J. Geophys. Res.* **69**, 1861–1874 (1964)
- A. Nishida, *Geomagnetic Diagnosis of the Magnetosphere* (Springer, New York, 1978)
- D.S. Ozturk, S. Zou, A.J. Ridley, J.A. Slavin, Modeling study of the geospace system response to the solar wind dynamic pressure enhancement on 17 March 2015. *J. Geophys. Res. Space Phys.* **123**, 2974–2989 (2018). <https://doi.org/10.1002/2017JA025099>
- E.N. Parker, Dynamics of the interplanetary gas and magnetic fields. *Astrophys. J.* **128**, 664–676 (1958)
- A.J. Ridley, A.D. Richmond, T.I. Gombosi, D.L. De Zeeuw, C.R. Clauer, Ionospheric control of the magnetospheric configuration: thermospheric neutral winds. *J. Geophys. Res.* **108**(A8), 1328 (2003). <https://doi.org/10.1029/2002JA009464>
- A.J. Ridley, D.L. De Zeeuw, W.B. Manchester, K.C. Hansen, The magnetospheric and ionospheric response to a very strong interplanetary shock and coronal mass ejection. *Adv. Space Res.* **38**, 263–272 (2006)
- C.T. Russell, M. Ginskey, Sudden impulses at low latitudes: transient response. *Geophys. Res. Lett.* **20**, 1015–1018 (1993)



- T. Saito, Geomagnetic pulsations. *Space Sci. Rev.* **10**, 319–412 (1969)
- A.A. Samsonov, D.G. Sibeck, Large-scale flow vortices following a magnetospheric sudden impulse. *J. Geophys. Res. Space Phys.* **118**, 3055–3064 (2013). <https://doi.org/10.1002/jgra.50329>
- A.A. Samsonov, D.G. Sibeck, J. Imber, MHD simulation for the interaction of an interplanetary shock with the Earth's magnetosphere. *J. Geophys. Res.* **112**, A12220 (2007). <https://doi.org/10.1029/2007JA012627>
- A.A. Samsonov, D.G. Sibeck, Y. Yu, Transient changes in magnetospheric–ionospheric currents caused by the passage of an interplanetary shock: northward interplanetary magnetic field case. *J. Geophys. Res.* **115**, A05207 (2010). <https://doi.org/10.1029/2009JA014751>
- A.A. Samsonov, D.G. Sibeck, N.V. Zolotova, H.K. Biernat, S.-H. Chen, L. Rastaetter, H.J. Singer, W. Baumjohann, Propagation of a sudden impulse through the magnetosphere initiating magnetospheric Pc5 pulsations. *J. Geophys. Res.* **116**, A10216 (2011). <https://doi.org/10.1029/2011JA016706>
- A.A. Samsonov, D.G. Sibeck, B.M. Walsh, N.V. Zolotova, Sudden impulse observations in the dayside magnetosphere by THEMIS. *J. Geophys. Res. Space Phys.* **119**, 9476–9496 (2014). <https://doi.org/10.1002/2014JA020012>
- A.A. Samsonov, V.A. Sergeev, M.M. Kuznetsova, D.G. Sibeck, Asymmetric magnetospheric compressions and expansions in response to impact of inclined interplanetary shock. *Geophys. Res. Lett.* **42**, 4716–4722 (2015). <https://doi.org/10.1002/2015GL064294>
- R. Selvakumaran, B. Veenadhari, Y. Ebihara, Sandeep Kumar, D.S.V.V.D. Prasad, The role of interplanetary shock orientation on SC/SI rise time and geoeffectiveness. *Adv. Space Res.* **59**(1425), 5 (2017)
- G.L. Siscoe, N.U. Crooker, G.M. Erickson, B.U.Ö. Sonnerup, K.D. Siebert, D.R. Weimer, W.W. White, N.C. Maynard, Global geometry of magnetospheric currents inferred from MHD simulations, in *Magnetospheric Current Systems*, ed. by S. Ohtani, R. Fujii, M. Hesse, R.L. Lysak (AGU, Washington, DC, 2000), pp. 41–52
- S.P. Slinker, J.A. Fedder, W.J. Hughes, J.G. Lyon, Response of the ionosphere to a density pulse in the solar wind: simulation of travelling convection vortices. *Geophys. Res. Lett.* **26**, 3549–3552 (1999)
- T.R. Sun, C. Wang, J.J. Zhang, V.A. Pilipenko, Y. Wang, J.Y. Wang, The chain response of the magnetospheric and ground magnetic field to interplanetary shocks. *J. Geophys. Res. Space Phys.* **120** (2015). <https://doi.org/10.1002/2014JA020754>
- T. Tamao, The structure of three-dimensional hydromagnetic waves in a uniform cold plasma. *J. Geomag. Geoelectr.* **16**, 89–114 (1964a)
- T. Tamao, A hydromagnetic interpretation of geomagnetic SSC. *Rep. Ionos. Space Res. Jpn.* **18**, 16–31 (1964b)
- T. Tamao, Transmission and coupling resonance of hydromagnetic disturbances in the non-uniform Earth's magnetosphere. *Sci. Rep. Tohoku Univ. Ser. 5 Geophys.* **17**, 43–72 (1965)
- T. Tanaka, M. Watanabe, M. Den, S. Fujita, Y. Ebihara, T. Kikuchi, K.K. Hashimoto, R. Kataoka, Generation of field-aligned current (FAC) and convection through the formation of pressure regimes: correction for the concept of Dungey's convection. *J. Geophys. Res.* **121** (2016). <https://doi.org/10.1002/2016JA022822>
- T. Tanaka, Finite volume TVD scheme on an unstructured grid system for three-dimensional MHD simulation of inhomogeneous systems including strong background potential fields. *J. Comput. Phys.* **111**, 381–389 (1994)
- T. Tanaka, Generation mechanisms for magnetosphere–ionosphere current systems deduced from a three-dimensional MHD simulation of the solar wind–magnetosphere–ionosphere coupling processes. *J. Geophys. Res.* **100**, 12057–12074 (1995)
- T. Tanaka, Configuration of the magnetosphere–ionosphere convection system under northward IMF conditions with nonzero IMF  $B_y$ . *J. Geophys. Res.* **104**, 14683–14690 (1999)
- T. Tanaka, Formation of magnetospheric plasma population regimes coupled with the dynamo process in the convection system. *J. Geophys. Res.* **108**(A8), 1315 (2003). <https://doi.org/10.1029/2002JA009668>
- T. Tanaka, Magnetosphere–ionosphere convection as a compound system. *Space Sci Rev* **133**, 1 (2007). <https://doi.org/10.1007/s11214-007-9168-4>
- T. Tanaka, Substorm auroral dynamics reproduced by the advanced global M–I coupling simulation, in *Auroral Dynamics and Space Weather, Geophys. Monogr. Ser.*, vol. 215, ed. by Y. Zhang (AGU, Washington D. C, 2015), p. 177
- S. Tsunomura, Numerical analysis of global ionospheric current system including the effect of equatorial enhancement. *Ann. Geophys.* **17**, 692–706 (1999)

- S. Tsunomura, T. Araki, Numerical analysis of equatorial enhancement of geomagnetic sudden commencement. *Planet. Space Sci.* **32**, 599–604 (1984)
- B.T. Tsurutani, W.D. Gonzalez, G.S. Lakhina, S. Alex, The extreme magnetic storm of 1–2 September 1859. *J. Geophys. Res.* **108**, 1268 (2003). <https://doi.org/10.1029/2002JA009504>. A7
- C.R. Wilson, M. Sugiura, Hydromagnetic interpretation of sudden commencements of magnetic storms. *J. Geophys. Res.* **66**(12), 4097–4111 (1961). <https://doi.org/10.1029/JZ066i12p04097>
- J. Wygant, F. Mozer, M. Temerin, J. Blake, N. Maynard, H. Singer, M. Smiddy, Large amplitude electric and magnetic field signatures in the inner magnetosphere during injection of 15 MeV electron drift echoes. *Geophys. Res. Lett.* **21**, 1739–1742 (1994). <https://doi.org/10.1029/94GL00375>
- Y. Yu, A.J. Ridley, The response of the magnetosphere-ionosphere system to a sudden dynamic pressure enhancement under southward IMF conditions. *Ann. Geophys.* **27**, 4391–4407 (2009)
- Y.-Q. Yu, A.J. Ridley, Understanding the response of the ionosphere-magnetosphere system to sudden solar wind density increases. *J. Geophys. Res.* **116**, A04210 (2011). <https://doi.org/10.1029/2010JA015871>
- K. Yumoto, V. Pilipenko, E. Fedorov, N. Kurneva, M. De Laetis, K. Kitamura, Magnetospheric ULF wave phenomena stimulated by SSC. *J. Geomag. Geoelectr.* **49**, 1179–1195 (1997)
- X.Y. Zhang, Q.-G. Zong, Y.F. Wang, H. Zhang, L. Xie, S.Y. Fu, C.J. Yuan, C. Yue, B. Yang, Z.Y. Pu, ULF waves excited by negative/positive solar wind dynamic pressure impulses at geosynchronous orbit. *J. Geophys. Res.* **115**, A10221 (2010). <https://doi.org/10.1029/2009JA015016>
- X. Zhou, B.T. Tsurutani, Interplanetary shock triggering of nightside geomagnetic activity: substorms, pseudobreakups, and quiescent events. *J. Geophys. Res.* **106**(A9), 18957–18967 (2001)
- X.-Y. Zhou, R.J. Strangeway, P.C. Anderson, D.G. Sibeck, B.T. Tsurutani, G. Haerendel, H.U. Frey, J.K. Arballo, Shock aurora: FAST and DMSP observations. *J. Geophys. Res.* **108**(A4), 8019 (2003). <https://doi.org/10.1029/2002JA009701>
- S. Zou, D. Ozturk, R. Varney, A. Reimer, Effects of sudden commencement on the ionosphere: PFISR observations and global MHD simulation. *Geophys. Res. Lett.* **44**, 3047–3058 (2017). <https://doi.org/10.1002/2017GL072678>

**Publisher's Note** Springer Nature remains neutral with regard to jurisdictional claims in published maps and institutional affiliations.

## Affiliations

Shigeru Fujita<sup>1,2</sup> 

✉ Shigeru Fujita  
sfujita@mc-jma.go.jp

<sup>1</sup> Meteorological College, Asahi 7-4-81, Kashiwa, Chiba 277-0852, Japan

<sup>2</sup> Space and Upper Atmospheric Research Group, National Institute of Polar Research, Midori 10-3, Tachikawa, Tokyo 190-8518, Japan